Electrochemical properties of carbon nanotubes/PANI/metal oxide nanoparticle nanocomposites towards electrocatalysis of some organochlorine pesticides

KK Masibi

orcid.org/0000-0002-2529-9016

Dissertation submitted in fulfilment of the requirements for the degree *Master of Science in Chemistry* at the

North-West University

Supervisor : Prof EE Ebenso

Co-Supervisors : Dr AS Adekunle

: Dr OE Fayemi

Graduation May 2018

Student number: 17113660

NWU®
NORTH-WEST UNIVERSITY
NOORDWES-UNIVERSITEIT
UNIBESITI YA BOKONE-BOPHIRIMA

DECLARATION

I Masibi Kgotla Katlego hereby declare that the work presented in this dissertation titled Electrochemical Properties of Carbon Nanotubes/PANI/Metal oxide nanoparticle Nanocomposites Towards Electrocatalysis of some Organochlorine Pesticides submitted to the North West University, Faculty of Agriculture, Science and Technology, Department of Chemistry, is my own work and has not been submitted for any degree or examination in any other university, and that all sources have been quoted, indicated and acknowledged by means of complete reference.

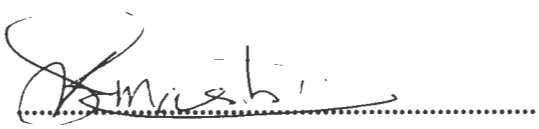

KGOTLA KATLEGO MASIBI

ABSTRACT

This work describes the chemical synthesis of antimony oxide nanoparticles (AONPs), polyaniline (PANI), acid functionalized single-walled carbon nanotubes (fSWCNTs) and the nanocomposite (AONP-PANI-SWCNT) as composite material for the trace detection of lindane and endosulfan (EDS). Successful synthesis of the nanomaterials was confirmed by fourier transform infrared spectroscopy (FT-IR), ultraviolet-visible (UV-Vis) spectrophotometry, x-ray diffraction (XRD) spectroscopy and scanning electron microscopy (SEM). Drop-cast method was used to modify glassy carbon electrode (GCE) with the synthesized nanomaterials. Electrochemical behaviour of the modified electrodes was explored using cyclic voltammetry (CV) and electrochemical impedance spectroscopy (EIS) using the ferricyanide/ferrocyanide ($[Fe(CN)_6]^{4-}/[Fe(CN)_6]^{3-}$) redox probe. AONP-PANI-SWCNT modified GCE exhibited faster electron transport properties as well as enhanced catalytic current response as compared to bare-GCE, GCE-AONPs, GCE-PANI, and GCE-SWCNT. Electrocatalytic studies further show that AONP-PANI-SWCNT modified GCE was stable with only a small current decrease between the 1^{st} and 20^{th} scan in both lindane and EDS. The fabricated sensor proved superior towards the detection of lindane as compared with literature reports yielding a low detection limit of 2.01 nM in the [lindane] range of 0 to 18.8 nM. The sensor also demonstrated good electrochemical properties toward Endosulfan (EDS) detection with a limit of detection (LoD) of 5.22 µM in the [EDS] range of 32.3 to 77.6 µM. CV and continuous aperommetry (CA) experiments were conducted to investigate the selectivity of the fabricated sensor. The results obtained indicated that the sensor is highly selective towards the detection of both lindane and endosulphan in the presence of various organic and inorganic interfering species. Real sample analysis was conducted on river water and tap water samples, the average recoveries were calculated and are indicative of the potential practical application for the proposed sensor.

ACKNOWLEDGEMENTS

I thank the almighty God for the gift of life. I thank my supervisor Prof. E. E. Ebenso for believing in a part time student and opening the doors of MaSIM research group for that I am grateful Prof. To My Co-Supervisors Dr. O.E. Fayemi and Dr. A.S. Adekunle thank you for your patience, support and guidance through this journey I have learned a lot from your teachings may God bless you.

I am grateful to the North West University Department of Chemistry staff and the MaSIM Research Group for all the assistance. You are greatly appreciated; Mr. Kagiso Mokalane, Mr. Sizwe Loyilane, Mr. Peter Mahlangu, Ms. Nomfundo Gumbi, Prof. Indra Bahadur, Dr. Lukman Olasunkanmi, Dr. Mwadham Kabanda, Ms. Pearl Seoposengwe, Mr. Thato Majele, Ms. Palesa Tsele, Mr. Mashuga Motsie, Mr. Henry Nwankwo, Mr. Gnanapragasam Raphael, Mr. Taiwo Quadri and Ms. Boikanyo Diseko.

Special thanks to Mr. Samuel Nde for assistance with acquiring the river-water samples. I am grateful to the NorthWest University for financial support.

To Mrs. Charmaine Masibi thank you my beloved wife for your support, encouragement and understanding. Special thanks to my son Oreutlwile Masibi, Kagiso Masibi, Tebogo Masibi, Boikobo Masibi, Ikgopoleng Masibi, Mpho Chenepe. Outmost appreciation to Matsheka, Molosiwa, Mooketsi, Motsusi and Makgoana families.

TABLE OF CONTENTS

LIST OF ABBREVIATIONS

AC	Alternating current
Ag	Silver wire pseudo-reference electrode
Ag/AgCl	Silver/Silver Chloride reference electrode
AO	Antimony oxide
CA	Continuous amperometry
CE	Counter electrode
CNTs	Carbon nanotubes
CV	Cyclic voltammetry
DDT	Dichlorodiphenyltrichloroethane
DET	Dissociative electron transfer
DMF	Dimethylformamide
DPV	Differential pulse voltammetry
EDS	Endosulfan
EIS	Electrochemical impedance spectroscopy
FT-IR	Fourier transform infrared
GC	Gas chromatography
GCE	Glassy carbon electrode
HPLC	High performance liquid chromatography
LoD	Limit of detection
LoQ	Limit of quantification
MWCNTs	Multi-walled carbon nanotubes
NPs	Nanoparticles
NPV	Normal pulse voltammetry
OCPs	Organochlorine pesticides
PAHs	Polycyclic aromatic hydrocarbons
PAN	Pesticide action network
PANI	Polyaniline
PBDEs	Polybrominated diphenyl ethers
PBS	Phosphate buffer solution
PCBs	Polychlorinated biphenyls
PCDDs	Polychlorinated dibenzo-p-dioxins
PCDFs	Polychlorinated dibenzofurans

POPs	Persistent organic pollutants
RE	Reference electrode
SCE	Standard calomel electrode
SEM	Scanning electron microscopy
SWCNTs	Single-walled carbon nanotubes
SWV	Square-wave voltammetry
UV-Vis	Ultraviolet-visible
WE	Working electrode
WHO	World health organization
XRD	X-ray diffraction
γ-HCH	γ-hexachlorocyclohexane

LIST OF SYMBOLS

α	Electron transfer coefficient
E	Potential
E^o	Standard cell potential
R	Universal gas constant
T	Absolute temperature
n	Number of electrons
F	Faraday constant
φ	Inner electric potential
A	Electroactive surface area (cm^2)
k_s	Standard rate constant of electron transfer
I_p	Peak current of redox couple
D	Diffusion coefficient
Z	Impedance
V	Voltage
I	Current
j	Imaginary factor
ω	Frequency
R_s	Solution resistance
C_{dl}	Double layer capacitance
R_{ct}	Charge transfer resistance
ω	Warburg impedance
Z`	Real impedance
Z``	Imaginary impedance
f	Frequency
Q	Charge
W	Warburg impedance
I_{pa}	Anodic peak current
v	Scan rate
V	Volts
Hz	Hertz

LIST OF FIGURES

LIST OF TABLES

LIST OF SCHEMES

CHAPTER 1

INTRODUCTION AND PROBLEM STATEMENT

1. Introduction and problem statement

1.1 Persistent organic pollutants

Post Second World War scientists realized that certain chemical pollutants were capable of persisting in the environment for a longtime, migrating from one environmental media to another.[1-6] These chemical pollutants by their nature and organic origin are called persistent organic pollutants (POPs)[1-6] and there are thousands of POP chemicals. The important classes of POP chemicals are mainly the families of chlorinated and brominated aromatics which include, polychlorinated biphenyls (PCBs), polychlorinated dibenzo-p-dioxins (PCDD's), polychlorinated dibenzofurans (PCDFs), polybrominated diphenyl ethers (PBDEs) and different organochlorine pesticides (OCPs).[2,3]

POP chemicals are hydrophobic and lipophilic.[1-6] They tend to resist photolytic, chemical and biological degradation and these properties afford them to have half-lives of decades in soils and sediments.[1-6] In aquatic environment, POPs possess the ability to partition into solids such as organic matter avoiding the aqueous phase.[2] They also partition into lipids avoiding the aqueous media of animal cells and become stored in fatty tissues, organs and muscles.[1,2] POPs can enter the gaseous phase under normal environmental temperatures.[2] As a result, they may undergo volatization from soils, vegetation and water into the atmosphere and through strong resistance to degradation they can travel over long distances in air before being re-deposited.[1,2] This ultimately results in widespread distribution of POPs even to areas where they were never used.[1-6]

Some POPs like PCDD/Fs are produced unintentionally as by products in the synthesis of some chemicals, however, many have been synthesized for industrial and agricultural uses.[2-5] Municipal waste may also contain POPs and other hazardous substances such as heavy metals, and polycyclic aromatic hydrocarbons (PAHs) all originating from materials such as batteries, used paints, oils, solvents, pesticides and other waste materials.[3-5]

1.1.1 Organochlorine pesticides

Generally, pesticides are widely used to control the growth and proliferation of undesirable organisms that, if left unchecked, would cause significant damage to forests, crops, stored food products, ornamental and landscape plants, and building structures.[7,8] Hence the use of pesticides in both agriculture and non-agricultural settings provides important benefits to society, contributing to an abundant supply of food and fiber and to the control of a variety of public health hazards and nuisance pests.[7,8] Owing to the fact that they are designed to be biologically active, pesticides have the potential to cause undesirable side effects. These include adverse health effects on farm workers, consumers of food products, and non-target wildlife organisms.[7,9,10] Deaths from exposure to pesticides are common; each year, tens of thousands of farmers especially in developing countries are affected. Earlier studies showed that approximately three million people are poisoned and two hundred thousand die from pesticide poisoning each year.[9] These figures must, however, be interpreted with caution, noting that not all hospital admissions and deaths were due to occupational poisoning but include cases of self-ingestion and accidental ingestion.[7] Furthermore, there is evidence suggesting that some pesticides may cause immune dysfunction, liver or kidney cancer, convulsions, headache, dizziness, nausea, vomiting, tremors, confusion, muscle weakness, slurred speech salivation and sweating.[7,9,10]

OCPs emanating from POPs are chlorinated hydrocarbons used extensively from early 1900 in agriculture and mosquito control.[11,12] Like POPs they accumulate in the environment and are very persistent.[1-6,11,12] Representative compounds in this group include, among many others dichlorodiphenyltrichloroethane (DDT), methoxychlor, dieldrin, chlordane, toxaphene, mirex, kepone, lindane, alanchlor, endosulphan, dicofol, heptachlor and benzene hexachloride.[1-3,5,11,12] The worldwide consumption of pesticides was at one time reported to have reached 2.6 million metric tons;[9] and of this total agricultural use accounting for 85 %.[11,9] Developed countries have the largest volume of consumption while developing countries have a rapidly growing use.[9] In addition to the increase in quantities of pesticides used, famers use stronger concentrations, they also increased the frequency of application and they tend to mix several pesticides together to combat pesticide resistance by pests.[9] These trends were particularly noticed in developing countries.[9] For the purpose of this study only some selected OCPs which are lindane and endosulphan was studied.

1.1.1.1 Lindane

Lindane (γ-hexachlorocyclohexane (γ-HCH)) is an organochlorine pesticide with molecular formula $C_6H_6Cl_6$ and molecular weight of 290.85 g/mol with melting point of 112°C – 113°C. Physically, lindane appears as a colourless-to-white powder with a musty odour.[12,13,16] Figure 1.1 shows the structural formula of lindane; the structure depicts a cyclohexane ring with chlorine atoms attached to each carbon atom of the ring. As a result lindane has eight known geometric isomers whose identification is based on axial or equatorial positions of the chlorine atoms around the cyclohexane ring. Out of these stereoisomers, only the γ-HCH exhibits insecticidal properties.[16] γ-HCH is known to be very volatile and when applied particularly to crops about 90% of the pesticide enters the atmosphere and is eventually deposited by rain.[13] Lindane is banned globally for agricultural use, however, the pesticide is still widely used in shampoos and lotions to treat head lice and scabies.[14-17] Lindane accumulation has been detected globally in human blood, breast milk, and adipose tissue.[16] Given its toxicity, lindane is linked to a number of adverse human health effects. These health effects include neurological effects such as seizures, convulsions, vertigo and elevated risks of liver and breast cancer. Most of the reported health effects have been related to agricultural use and chronic occupational exposures.[13-17]

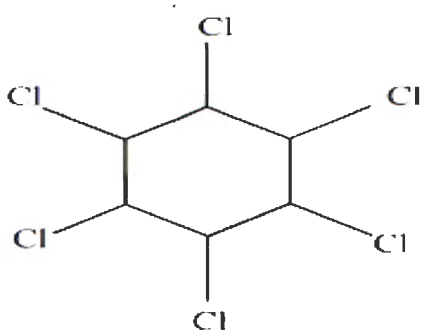

Figure 1.1: Lindane structure[1]

1.1.1.2 Endosulfan

Endosulfan (6,7,8,9,10,10-hexachloro-1,5,5a,6,9,9a-hexahydro-6,9-methano-2,4,3-benzodioxathiepin-3-oxide) is a broad spectrum organochlorine insecticide primarily used on a variety of cereals, fruits, vegetables and cotton.[18-22] It has a molecular formula $C_9H_6Cl_6O_3S$ and molecular weight of 406.93 g/mol with melting point of 208°C –210°C. Physically it

appears as a cream-to-white solid that may appear crystalline or in flakes and it has a distinct odour similar to turpentine. It is sold as a mixture of its two isomers α- and β-endosulfan in a ratio of 7:3 respectively,[18,20-22] Figure 1.2 shows the structural formula of endosulfan (EDS) and its two isomers. PAN (pesticide action network) reported EDS as the world's most widespread pollutant; it is also reported as a widespread contaminant of human breast milk found in samples from women in Egypt, Madagascar, South Africa, Denmark and many other countries.[17] Effects of EDS exposure include convulsions, psychiatric disturbances, epilepsy, paralysis, impaired memory, immunosuppression, neurological disorders and death.[17,18] Neurotoxicity is the major endpoint of concern in human beings and experimental animals. The subacute and chronic toxicity studies of EDS in animals suggested that the liver, kidneys, immune system and testes are the main target organs.[18] No data is available for subacute or chronic exposure to EDS in human subjects.[18]

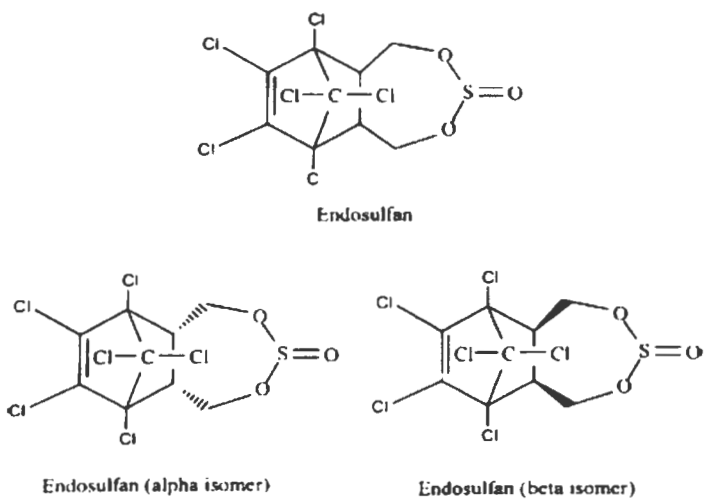

Figure 1.2: Endosulfan and its two isomers[23]

1.2 Problem statement

The presence of OCPs in the environment is of great concern due to their toxic effects on humans and other organisms.[7] These pollutants require constant monitoring which is currently underprovided in South Africa.[9] Conventional analytical methods such as gas chromatography (GC) and high performance liquid chromatography (HPLC) are expensive, sophisticated and require time consuming sample preparations,[2,7] therefore, there is a need for the development of simpler yet effective methods.

1.3 Aims and objectives of study

The aim of the study is to explore the sensing properties of carbon nanotubes/PANI/Metal-oxide nanocomposites towards the detection and quantification of some selected organochlorine pesticides.

1.4 The specific objectives are to:

- Synthesize polyaniline (PANI) and antimony oxide (AO) nanoparticles (NPs)
- Treat single-walled carbon nanotubes (SWCNT) with acid.
- Fabricate nanocomposite from the synthesized PANI, AONPs and SWCNT.
- Fabricate a sensor by modifying glassy carbon electrode with the synthesized nanocomposite.
- Explore the sensing properties of the modified sensor (electrode) towards the selected organochlorine pesticides using electrochemical techniques.
- Explore the stability of the modified sensor towards the analytes
- Determine the sensor's limit of detection (LoD) for each analyte
- Carry out real sample analysis to establish the analytical application of the developed sensor in environmental matrices.

1.5 Research justification

Scientific and medical journals increasingly report the risks posed to human health by pesticides including links between pesticides and diseases such as cancer and hormone disruptions.[7] In South Africa, The Fertilizers, Farm Feeds, Agricultural Remedies and Stock Remedies Act, 1947 (Act No. 36 of 1947) is over 60 years old.[7] Changes to the context within which pesticides are managed, have taken place and have led to a need to consider reviewing the current act in order to improve efficiency and effectiveness of pesticides management in South Africa and the world in general.[7] Among others, the act does not adequately incorporate international obligations to which South Africa is a party. There is lack of establishment of pesticide use surveillance and monitoring systems, as this can be used to gather information on common conditions of use and their impact on health and environment.[7] From the above, it can be said that there is no proper monitoring of these important environmental pollutants hence

the need for the development of devices that can be readily and effectively used for the purpose of monitoring such environmental pollutants. This study, therefore, aims at fabricating very cheap, miniaturised electrochemical sensor using nanocomposite based materials for routine check and balances in the levels of OCPs in water, soil, sediments and other environmental matrices.

CHAPTER 2

LITERATURE REVIEW

2. Literature review

2.1 Metal, metal-oxide nanoparticles in sensors

Nano is a prefix like micro, pico and so forth, used in front of a microscopic unit to change its value by orders of some magnitude.[24] Nano equates to one billionth (10^{-9}) thus a nanometer is a billionth of a meter. [24] Nanoparticles (NPs) can be defined as particulate dispersions or solid particles of size range of 1-1000 nm and include nano-scale metals, semiconductor metals and metal oxides. These novel materials are known to exhibit very interesting physical characteristics relating to, or as a result of the changes in electronic structure as well as large surface to volume ratios which make them much different from their corresponding bulk materials.[26] These fascinating characteristics include unique mechanical strength, light absorbing and emitting properties, magnetism and good conductivity.[24-27] These novel and intrinsic properties of nanoparticles as well as their low cost and their ability to be incorporated into a variety of matrices to form nanocomposite films is attracting much attention to researchers.[24-25] There is a vast literature available on the use of metal, metal oxide nanoparticles in sensors, particularly for trace detection of environmental pollutants and other significant materials. Abodollah Salimi et al.[28] reported the successful synthesis of a novel cobalt oxide NPs based sensor by modifying glassy carbon electrode (GCE) with cobalt oxide NPs for the detection of trace amounts of arsenic using cyclic voltammetry (CV) experiments. Authors reported a detection limit of 11 nM consequently recommending the fabricated sensor for real sample analysis noting the world health organization (WHO)'s 100 nM guideline value of arsenic in drinking water.[28] Camelia Grosan et al.[29] fabricated a novel modified electrode by linking leucine capped gold NPs to 1,3-propanedithiol self-assembled monologue on a gold substrate. This nanostructured assembly was tested for detection of Cu(II) ions using cyclic voltammetry and a detection limit of 5.4×10^{-7} M was reported. [29] Stephen Mailu et al.[30] fabricated a novel electrochemical sensor for the detection of anthracene by modifying GCE with over-oxidized polypyrrole(PPyox) and Ag-Au bimetallic NPs. PPyox was over-oxidized to avoid electrode fouling as it is one of the challenges in the determination of polyaromatic hydrocarbons. Authors described some linear relationship between anodic current and anthracene concentration over the range of 3.0×10^{-6} to 3.56×10^{-4} M with a detection limit of 1.69×10^{-7} M.[30] Table 1 below summarizes some reported literature on the use of metal, metal oxide nanocomposites in the detection of some important analytes using electrochemical methods.

Table 2.1: Literature on the use of metal, metal oxide nanocomposites for detection of some important analytes.

Composite electrode	Method used	Analyte	LoD (nM)	Reference
Co_3O_4NPs/GCE	**CV**	**As^{3+}**	**11**	**[28]**
Leucine-AuNPs/Au electrode	CV	Cu^{2+}	0.054	[29]
Ppyox/Ag-AuNPs/GCE	**CV**	**Anthracene**	**0.0169**	**[30]**
MIP/NiNPs/GP/CE	CV	TBBPA	13	[31]
GCE/MWCNTs/NiONPs	**CV**	**Dopamine**	**7990**	**[32]**
GCE/MWCNTs/ZnONPs	CV	Dopamine	0.0374	[32]
GCE/MWCNTs/Fe_3O_4NPs	**CV**	**Dopamine**	**0.0014**	**[32]**
AgNPs/MWCNTs/GCE	CV, DPV	CZP	6	[33]
AgNPs/CNT	**ASSWV**	**As^{2+} and Pb^{2+}**	**43.8**	**[34]**
AgNPs/CNF	ASSWV	As^{2+} and Pb^{2+}	18.5	[34]
AuNPs/Ch/GCE	**CV, DPV**	**Nitrite**	**100**	**[35]**
AuNPS/P3MT/GCE	CV, Amperometry	Nitrite	230	[36]
AuNPS/P3MT/GCE	**CV, Amperometry**	**Iodate**	**140**	**[36]**
AuNPs/GCE	DPASV	Cd^{2+}, Pb^{2+}, Cu^{2+} and Hg^{2+}	300	[37]
GCE/α-MnO_2/NW	**CV, DPV, Amperometry**	**Lindane**	**114**	**[38]**
GCE/$NiCo_2O_4$	CV, DPV,	Lindane	3600	[16]
GCE/Nylon6,6/MWCNT/Fe_3O_4	**CV, SWV**	**Lindane**	**32**	**[39]**
Paraffin/MWCNT/SbNPs	CV, DPV	SMX	24	[40]
Paraffin/MWCNT/SbNPs	**CV, DPV**	**TMP**	**31**	**[40]**

Abbreviations: Ppyox – Polypyrole, MIP – Molecular imprinted polymer, GP – Graphene, CE – Carbon electrode, TBBPA – Tetrabromobisphenol A, MWCNTs – Multiwalled carbon nanotubes, CZP – Clonazepam, CNT – Carbon nanotube, ASSWV – Anodic striping with square wave voltammetry, CNF – Carbon nanofiber, Ch – Choline Chloride, DPASV – Differential pulse anodic stripping voltammetry, DPV – Differential pulse voltammetry, P3MT – Poly(3-Methylthiophene), NW – Nanowire, SWV – Square-wave voltammetry, SMX – Sulfamethoxazole, TMP – Trimethoprim

2.1.1 Antimony nanoparticles and their applications

Owing to their intrinsic properties such as negative over potential to hydrogen evolution, large scan potential range antimony (Sb) based electrodes have received growing attention in electrochemistry.[41] Sb has similar properties to bismuth and can act as a mercury free electrode in heavy metals striping analysis. Among all these characteristics there are a number of reports describing the use of electrodes based on antimony. Sb-powder-modified carbon paste electrode for determination of heavy metals,[41] amorphous carbon-coated Sn-Sb particles as anode material for lithium ion batteries[41] and Sb-film electrode plated over GCE for determination of sulfasalazine.[41]

2.1.2 Antimony oxide nanoparticles and their applications

Semi-conductor metal oxide nano-materials such as AONPs have given rise to an interesting area of research and technological application.[42-44] Researchers have focused a lot of efforts on synthesis, structure, properties and applications. It is reported that AONPs are key among all the other metal oxides from group V to group VI of the periodic table.[42] As compared to bulk AO, AONPs have a higher refractive index, higher abrasive resistance, higher proton conductivity, outstanding mechanical strength and higher absorbability.[42-45] The unique properties of AONPs have been explored in three different fields of application which are: chemical, sensing and semiconductors. With regard to the chemical field AONPs together with halogenated compounds are useful as flame retardants in plastics, paints, adhesives, sealants, rubber and textile.[42-45] In the field of sensors, most researchers primarily reported AONPs as promising material for humidity sensing given its high proton conductivity. Extremely fine particles of colloidal AONPs are used as optical materials due to their high refractive index and high abrasive resistance in the semiconductor field.[42-44]

However, from the literature studied, the use of SWCNTs/AONPs, PANI/AONPs or AONP/PANI/SWCNT nanocomposite modified electrodes in electrochemical sensors has not been reported. Furthermore, based on the characteristics of AONPs and electronic properties of both SWCNTs and PANI, the nanocomposites SWCNTs/AONPs, PANI/AONPs and AONP/PANI/SWCNT yields a very promising electrodic material for use in the development of electrochemical sensors.[44]

In constructing electrochemical sensors for environmental monitoring, NPs are mostly used in two ways. Firstly together with an enzyme (enzymatic sensors) to increase the rate of electron transfer and to improve the sensitivity of the sensor and secondly as an individual catalyst (non-enzymatic sensors) to catalyze the reactions and to lower the limit of detection.[18] For the purpose of this work, the latter will be explored.

2.2 Carbon nanotubes

From the Rice University in the mid-1980s, Smalley and co-workers[46] developed the chemistry of fullerenes. Fullerenes are geometric cage-like structures of carbon atoms composed of hexagonal and pentagonal faces. This discovery as well at the discovery of graphene led to the synthesis of carbon nanotubes (CNTs).[46,47] Nanotubes can be described as long, thin fullerenes where the walls of the tubes are hexagonal carbons (graphite structure) or simply as tubes made up of rolled graphene sheets and depending on whether the tube like structures are made up of single or multiple wells, the nanotube are known either as single-walled or multi-walled respectively. This is depicted by Figure 2.1 showing a single sheet of graphene rolled up to yield SWCNTs and multiple graphene sheets rolled up to yield multi-walled carbon nanotubes (MWCNTs). These novel materials (carbon nanotubes) have been shown to exhibit unique mechanical, electrical and thermal properties mostly derived from graphene and can be very useful in engineering development and many other fields.[47,48,49] The unique properties include high chemical stability, good electrical conductivity, high surface-volume ratio and high adsorption capacity of CNTs make them extremely attractive for use as support material in electrochemical sensors.[50]

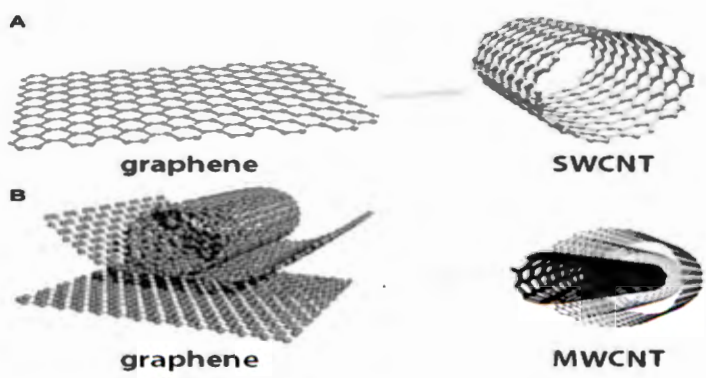

Figure 2.1: Carbon nanotubes[51]

SWCNTs are the strongest known material 100's of times stronger than the highest grade of high carbon steel commercially available.[52] Given the high surface area of SWCNTs and the fact that all of the carbon atoms in SWCNTs are surface atoms, they are an ideal support-material for metal NPs taking into account the low reactivity of sp^2 hybridized carbon atoms.[51] The substrates for supporting metal NPs have a considerable influence on their morphology and properties.[52] The use of SWCNTs as a supporting material for surface modification of electrodes in electrochemical studies of some important analytes include, nitrite electrochemical sensor based on Prussian blue/single-walled carbon nanotubes modified pyrolytic graphite electrode,[53] electrocatalytic detection of dopamine at single-walled carbon nanotubes-iron(III) oxide nanoparticles platform,[54] probing the electrochemical behavior of SWCNT-cobalt nanoparticles and their electrocatalytic activities towards the detection of nitrite at acidic and physiological pH conditions.[55]

2.3 Conducting polymers in sensors

Conducting polymers contain π-electron back bones responsible for their unusual electronic properties such as electrical conductivity, low energy optical transitions, low ionization potential and high electron affinity.[56] Commonly used conducting polymers in sensors include PANI, polypyrrole, polyacetylene, polyphenylene, and polythiophene.[56] PANI has attracted great attention due to a good combination of properties that include low cost, ease of synthesis, environmental and thermal stability, adequate electrical conductivity, wide application potential as well as oxidation or protonation adjustable electro-optical properties.[57-59] Since its discovery, PANI has exhibited various potential applications such as rechargeable batteries,[60] gas separation devices,[61] molecular sensors, light-emitting diodes,[62] and electrorheological material.[63] In the past two to three decades, PANI has emerged as one of the most interesting material for the fabrication of electrochemical sensors since it has the potential to exhibit improved sensor response and sensitivity.[63] Literature on the use of PANI based electrochemical sensors for electrochemical studies of environmentally important analytes is surprisingly very limited, however, some of the reported work include, a sensor for the determination of lindane using PANI/Zn, Fe(III) xides and Nylon 6,6/MWCNT/Zn, Fe(III) Oxide Nanofibers Modified Glassy Carbon Electrode,[39] graphenated polyaniline-doped tungsten oxide nanocomposite sensor for real time determination of phenanthrene,[57]

2.4 Electrochemical sensors

An electrochemical sensor is simply defined as a device that can provide continuous information about its environment by producing a certain type of response directly related to the quantity of a specific chemical species within a complex sample matrix.[65,66] In general, an electrochemical sensor comprises of two main component namely, one receptor which transforms the chemical information into a form of energy and one transducer part which transforms this energy into an analytically useful signal. [65,66] Figure 2.2 illustrates the basic components of an electrochemical sensor.

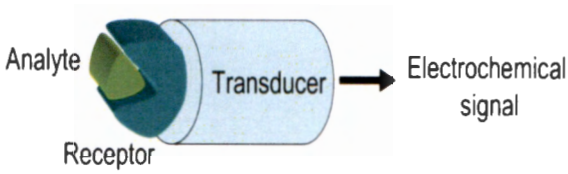

Figure 2.2: Electrochemical sensor[66]

Electrochemical sensors are known to offer a vast number of advantages as compared to conventional analytical methods such as UV-visible and infrared spectrophotometry, atomic absorption spectrophotometry, flourometry, mass spectrometry and chromatography which are expensive, complex, require skilled personnel, time consuming sample preparations and not suitable for onsite monitoring. Chemical sensors have no such requirements, they are inexpensive, suitable for onsite monitoring, non-destructive, adaptable to small sample volumes and they offer reproducible, fast and accurate responses. [39,38,65-67] There are mainly three types of electrochemical sensors namely; potentiometric, voltammetric and conductometric. In potentiometric sensors, an equilibrium is established at the sensor interface and either the electrode or membrane potential is measured and information about composition of a sample is obtained from the potential difference between two electrodes. In voltammetric sensors, a potential is applied between a reference and working electrode which then induces the oxidation or reduction of an electroactive species, the resultant current is then measured. Conductometric sensors are primarily involved with the measurement of conductivity at a series of frequencies; they rely on changes of electric conductivity of a film or bulk material whose conductivity is affected by the analyte present.[65] This study explores the prospect of the fabrication of a sensor based on voltammetric measurements.

2.5 Voltammetric techniques

Voltammetry is essentially based on the application of a time dependent potential to an electrochemical cell, the resulting current as a function of that potential is then measured. The resulting plot of current versus applied potential is called a voltammogram and it provides essential qualitative and quantitative information about the species involved in the reduction or oxidation (redox) reaction of interest. A basic voltammetric experiment is ideally carried out in a simple electrochemical cell consisting of three electrodes, namely working electrode (WE), reference electrode (RE) and counter electrode (CE) connected to a potentiostat. Figure 2.3 depicts a typical three electrode chemical cell.[68-70]

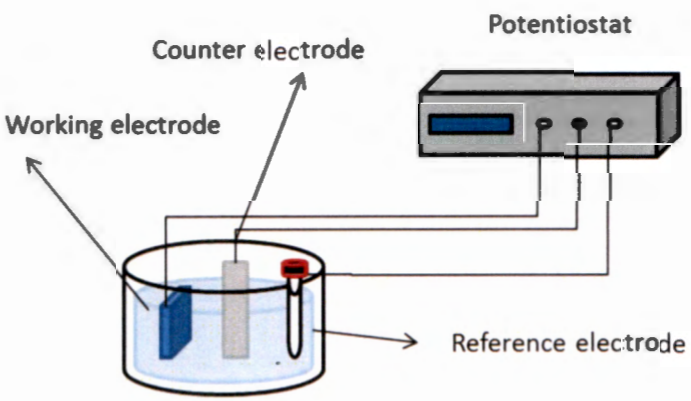

Figure 2.3: Typical electrochemical cell[71]

The WE acts as an electron conductor at which the redox reaction takes place. A counter reaction to that of the WE takes place at the CE so as to balance the total charge of the system. The RE is an electrode whose potential is known and kept constant for it is used as a reference against which the potential at other electrodes is measured. The main function of the potentiostat is to supply required voltage to the system and consequently record the current change in the system. The redox reaction taking place at the surface of the WE at the appropriate applied potential results in the mass transport of new material to the electrode surface and the generation of current directly proportional to the concentration of the analylyte.[68-70] Considering a simple electrochemical redox reaction such as $O + ne \leftrightarrow R$ the relationship between applied potential and the surface concentration of the redox species can be represented by the Nernst equations (equation 2.1),

$$E = E° - \frac{RT}{nF} ln \frac{[R]}{[O]} \quad (2.1).$$

Where R is the universal gas constant (8.314 J/molK), T is the absolute temperature (K), n is the number of electrons exchanged, F is the Faraday constant (96.485 C/mol), E° is the standard cell potential. If the potential applied to the electrode is changed, the ratio [R]/[O] at the electrode surface will also change so as to satisfy equation 1.[68-70]

The Butler-Volmer equation (equation 2.2) also links the variables for current, potential and concentration.

$$\frac{I}{nFA} = k_s e^{-\alpha\varphi} \{[R] - e^{\varphi}[O]\} \quad (2.2).$$

Where $\varphi = nF(E - E°)/RT$, k_s is the standard rate constant of electron transfer, α is the electron transfer coefficient and A is the electroactive surface area of the WE. Commonly known voltammetric techniques include CV and pulsed voltammetry. Pulsed voltammetric techniques are divided into numerous classes of techniques depending on the pulse wave form and the way by which the current is sampled and they are; Normal pulse voltammetry (NPV), differential pulse voltammetry (DPV) and square-wave voltammetry (SWV). For the purpose of this study only CV and SWV will be further explored.[68-70]

2.5.1 Cyclic voltammetry

CV is one of the most widely used electrochemical technique, almost all electrochemical studies begin with the application of CV.[68-70,72] The shape, position and time behaviour of the experimental voltammogram offers immediate analysis of electrochemical systems. On a quick inspection of a cyclic voltammogram, one may deduce information about the diffusive or adsorptive nature of the electrode process, reaction kinetics, thermodynamic parameters and both the existence and characteristics of coupled homogeneous chemical reactions.[72] This technique is based on ranging the applied potential at the WE in both the forward and reverse scan whilst monitoring the current. For an electrochemically reversible reaction, the response obtained from CV experiment is a simple voltammogram as shown in Figure 2.4.

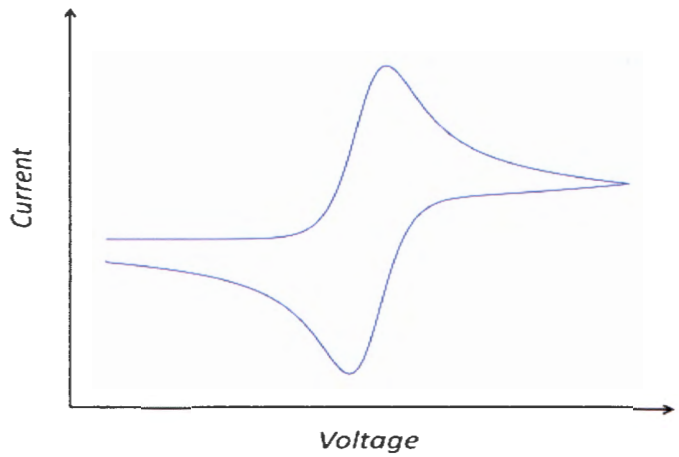

Figure 2.4: Typical cyclic voltammogram[73]

The concentration of the electroactive species can be linked to the peak current (I_p) by the Randles-Sevčik equation (equation 2.3) at 25°C.[68,70]

$$I_p = 2.69 \times 10^5 n^{3/2} AC\sqrt{Dv} \qquad (2.3).$$

Where I_p is the peak current of the redox couple, n is the number of electrons participating in the redox reaction, A is the electroactive surface area (cm^2), D is the diffusion coefficient redox species ($cm^2\ s^{-1}$), C is the concentration of redox species in the bulk solution (mol cm^{-3}) and v is the scan rate ($V\ s^{-1}$).

2.5.2 Square-wave voltammetry

SWV is considered one of the most advanced electroanalytical techniques known to combine the advantages of pulsed techniques, CV and impedance techniques thereby providing enhanced sensitivity, mechanistic insight into electrode processes and electro-kinetic measurements. In SWV, the potential applied consists of symmetrical square-wave pulses with constant amplitude (E_{sw}), these are then superimposed on a staircase-wave form as shown on Figure 2.5 (a) the resulting voltammogram is depicted by Figure 2.5 (b). In this technique, the current is measured twice, first at the end of the oxidation half cycle to give the corresponding oxidation current response then at the end of the reduction half cycle to give the reduction current response. The net current is then obtained from the subtraction between the oxidation and reduction currents, but this is ultimately the sum of the currents since the reduction current

by convention are negative. This is what makes SWV the most sensitive electroanalytical technique, like other voltammetric techniques the net peak current is proportional to the concentration of the electroactive specie resulting in detection limits in sub-nanomolar ranges.[68,74,75]

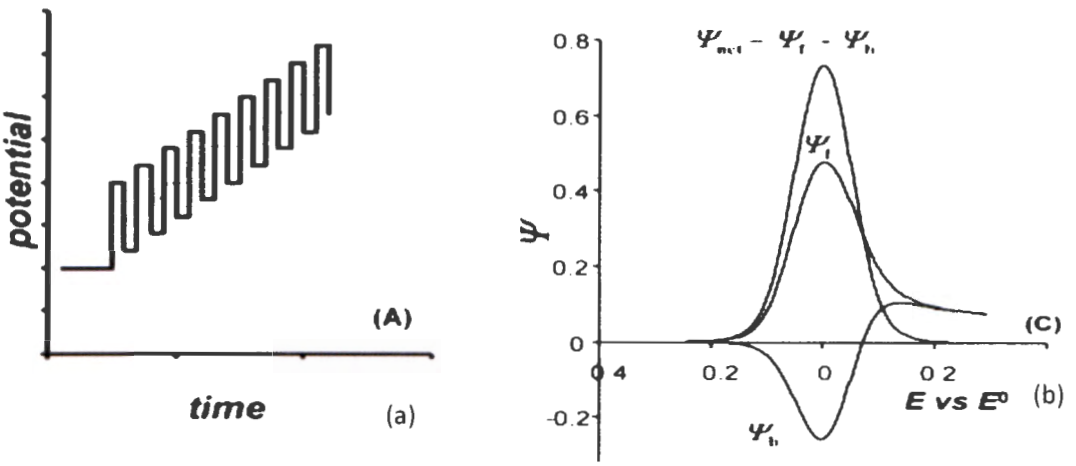

Figure 2.5: (a) Typical square-wave form in SWV (b) Typical square-wave voltammogram[74,75]

2.6 Electrochemical Impedance Spectroscopy

Electrochemical Impedance spectroscopy (EIS) is one of the most powerful and valuable methods in electrochemical research. The method is used to characterize electrode processes and complex interfaces.[76-78] EIS has had a wide range of applications such as elucidation of corrosion mechanisms, characterization of charge transport across membranes and membrane/solution interface, the optimization of batteries and fuel cells and of recent decades is the characterization of surface modifications of electrodes[77,78] which is of great importance particularly to this study. EIS is based on complex mathematical transforms first described by a valued mathematician Oliver Heaviside in the late 19th century to yield real values of impedance in temporal space. Heaviside defined impedance of a system as the complex ratio of the voltage and current in an alternating current (AC) circuit[78] and is determined by applying a voltage perturbation with a small amplitude and measuring the current response, [77] this is denoted by equation 2.4,

$$Z(j\omega) = \frac{V(j\omega)}{I(j\omega)} \qquad (2.4).$$

Where Z is impedance, V is the voltage, I is the current, j is the imaginary factor and ω is the frequency. To determine true values for the impedance requires manipulation of complex numbers, this is achieved from the impedance data normally obtained by running EIS experiments and employing complementary software. The data can be presented in the form of Nyquist plot where real and imaginary impedance components are plotted against one another; this is depicted by Figure 2.6 showing a simple Randles equivalent circuit for an electrochemical cell comprising of solution resistance (R_s), double layer capacitance (C_{dl}), charge transfer resistance (R_{ct}) and the Warburg impedance (ω).[77,78]

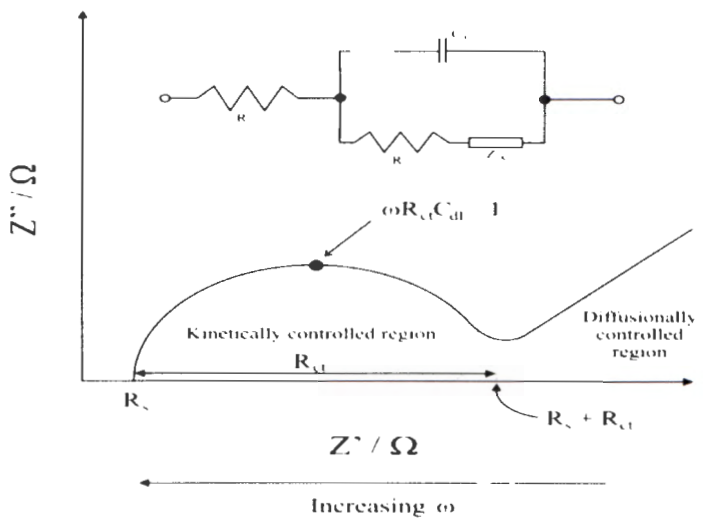

Figure 2.6: Randles equivalent circuit for an electrochemical cell[77,78]

C_{dl} can be calculated from the frequency at the maximum of the semicircle using equation 2.5.[76]

$$\omega = 2\pi f = 1/R_{ct}C_{dl} \quad (2.5).$$

The real (Z') and imaginary (Z'') impedances of the most common Nyquist plots are described by two fundamental equations,[78] equation 2.6 and equation 2.7.

$$Z' = R_s + R_{ct}/1 + \omega^2 R_{ct}^2 C_{dl}^2 \quad (2.6)$$

$$Z'' = R_{ct}^2 C_{dl}\omega/1 + \omega^2 R_{ct}^2 C_{dl}^2 \quad (2.7).$$

In bode plots the impedance and phase angle is plotted against frequency, this can be essential in determining the capacitative or inductive effects of electrochemical systems.[78]

CHAPTER 3

EXPERIMENTAL PROCEDURES

3. Experimental procedure

3.1 Materials and reagents

Pristine single wall carbon nanotubes (90% purity, 0.7-1.1 nm), tetrabutylammonium bromide (TBAB), Lindane ($C_6H_6Cl_6$), Endosulphan ($C_9H_6Cl_6O_3S$) and N,N-Dimethylformamide (DMF) were purchased from Sigma-Aldrich. Methanol, nitric acid (HNO_3), antimony chloride ($SbCl_3$), polyvinyl alcohol (PVA), sodium hydroxide (NaOH), hydrochloric acid (HCl), aniline (99%), ammoniumperoxodisulfate (APS) [$(NH_4)_2S_2O_8$], Sodium phosphate (NaH_2PO_4), Potasium phosphate (Na_2HPO_4), and ethanol were purchased from Merck chemicals (South Africa). Glassy carbon electrode (GCE, 3 mm diameter), Silver-silver chloride (Ag|AgCl) in saturated KCl reference electrode and platinum disk counter electrode were purchased from CH Instruments Inc., US. Polishing pads were obtained from Buehler, IL, USA and alumina micro powder (1.0, 0.3 and 0.05 μm alumina slurries) was used for polishing the glassy carbon electrode.

Ultrapure water of resistivity 18.2 MΩcm was obtained from a milli-Q Water System (Millipore Corp., Bedford, MA, USA) and was used throughout for the preparation of solutions. 0.1 M phosphate buffer solution (PBS) of pH 7.0 was prepared with appropriate amounts of NaH_2PO_4 and Na_2HPO_4 and adjusted with NaOH. Prepared solutions were purged with nitrogen to eliminate oxygen and prevent any form of oxidation during electrochemical experiments.

3.2 Instruments

Autolab Potentiostat PGSTAT 302 (Eco Chemie, Utrecht, and The Netherlands) driven by the GPES software version 4.9, UV-1901 UV-vis spectrophotometer (Agilent Technology, Cary series UV-vis spectrophotometer) using quartz cell with path length of 1.0 cm, Fourier transformed infrared spectrometer (Agilent Technology, Cary 600 series FTIR spectrometer, USA), high resolution scanning electron microscope (Zeiss Ultra Plus 55 HRSEM, Germany), X-ray diffraction spectrophotometer (Bruker-AXS, Madison, Wisconsin).

3.3 Synthesis of antimony oxide nanoparticles (AONPs)

Reported procedure was utilized as follows[43]. About 228 mg $SbCl_3$ was dissolved in 100 mL 1 M HCl, then 3 g of PVA was added. The mixture was dispersed by bath sonication for 15 minutes. Therefore, 12 mL of 10 M NaOH was added slowly to the mixture from a burette. The mixture gave a transparent yellow colour. The mixture was then refluxed for 1 hour and the colour became more intense. The mixture was heated at 350°C for 1 hour and the dry powder samples were obtained.

3.4 Synthesis of polyaniline

Polyaniline (PANI) was synthesized using a method described by Kavitha et al.[79] Two milliliter aniline and 50 mL 1 M HCl were added into a 250 mL beaker equipped with a magnetic stirrer at a temperature of 0°C. Five grams of APS aqueous solution in 50 mL 1 M HCl was added drop wise to the above solution. The polymerization temperature of 0°C was maintained for 10 hours to complete the reaction. The precipitate obtained was then filtered and washed successively with 1 M HCl followed by double distilled water until the wash solution turned colourless. The product was dried at 60°C for 24 hours to get powder form of PANI.

3.5 Synthesis of functionalized single-walled carbon nanotubes (fSWCNTs)

Single-walled carbon nanotubes (SWCNTs) were functionalized by modifying a reported procedure.[80] Forty milligram pristine SWCNTs were first dispersed in 40 mL DMF by bath sonication for 40 minutes at 40°C. This dispersion was then filtered and washed on the filter with 10 mL methanol followed by deionized water. The solid was transferred into a glass vial containing 20 mL 8 M HNO_3 and sonicated for 30 minutes at 40°C. The mixture was diluted with 40 mL deionized water and filtered. The solid material on the filter paper was washed with deionized water until the filtrate was neutral and finally washed with 10 mL of methanol and 10 mL of DMF. Lastly, the solid was dispersed in 20 mL DMF by bath sonication for 60 minutes at 40°C then filtered and dried to get powder form of fSWCNTs.

3.6 Electrode modification

The electrode was modified by the drop-cast method.[26,81] GCE surface was first cleaned by gently polishing it with 0.3 μm alumina slurries on a carborundum paper followed by a mirror finish on a Buehler felt pad. The electrode was then rinsed thoroughly with double distilled water, followed by ultrasonic vibration and left for 5 minutes in ethanol and water. About 5 mg each of the prepared nanomaterials, AONPs, PANI, fSWCNTs and a combination of 5 mg each of the nanomaterials were suspended in 1 mL DMF. Each suspension was then dispersed by ultrasonic vibration for 30 minutes, and a 20 μL aliquot of this dispersion was dropped onto the GCE surface and dried at 50°C to obtain the modified electrodes.

3.7 Characterization

3.7.1 Structure and morphology

Fourier transform infrared spectroscopy (FT-IR), Ultraviolet-visible (UV-Vis) spectrophotometry, X-ray diffraction (XRD) spectroscopy and Scanning electron microscopy (SEM) were used for the structural and morphological characterization of the synthesized nanomaterials. The results obtained for the synthesized AONPs, PANI, fSWCNTs and the composite AONP/PANI/SWCNT are discussed in chapter 4.

3.7.2 Electrochemical characterizaion

Electrochemical experiments were carried out to establish both the successful modification of the GCE and the electron transport kinetics of GCE and modified GCE. Cyclic voltammetry (CV) and electrochemical impedance spectroscopy (EIS) were employed to obtain the electrochemical measurements.

3.7.2.1 Cyclic voltammetry

Cyclic voltammetry (CV) experiments were carried out by running the bare GCE and various (AONPs, PANI, fSWCNTs and AONP/PANI/SWCNT) GCE modified electrodes first in 0.1 M phosphate buffer solution (PBS) then in 5 mM $[Fe(CN)_6]^{4-/3-}$ solution prepared in 0.1 M PBS at a scan rate of 25 mVs^{-1}. The GCE and the various nanoparticles (AONPs, PANI, fSWCNTs

and AONP/PANI/SWCNT) GCE modified electrodes were used as the working electrode, platinum wire as the counter electrode and Ag/AgCl, sat'd KCl as the reference electrode. The electroactive surface area of the modified electrodes was then determined from the data obtained.

3.7.2.2 Electrochemical impedance spectroscopy

Electrochemical impedance spectroscopy (EIS) experiments were carried out by running the bare GCE and various nanoparticles (AONPs, PANI, fSWCNTs and AONP/PANI/SWCNT) GCE modified electrodes first in 0.1 M PBS then in 5 mM $[Fe(CN)_6]^{4-}/[Fe(CN)_6]^{3-}$ solution ($E_{1/2}$ 0.2 V vs Ag/AgCl in sat'd KCl) between 100 kHz and 0.1 Hz using a 5 mV rms sinosoidal modulation. The results obtained were presented by Nynquist plots and fitted with a particular equivalent circuit. Charge transfer resistance (R_{ct}) values were determined from the EIS fitting.

3.8 Electrocatalytic studies

3.8.1 Lindane

The electrocatalytic reduction of lindane was investigated using CV in the presence of 9 μM lindane prepared in 60:40 methanol/water containing 0.05 M TBAB as supporting electrolyte. CV experiments were performed in the potential range -1.7 V to -0.2 V at a scan rate of 25 mVs^{-1}. A comparative study of the electrocatalytic behavior of the different modified electrodes towards lindane was investigated. Stability study as well as scan rate study of the modified electrode was also investigated. Electrochemical parameters such as peak current (I_p), peak potential (E_p), formal redox potential ($E_{1/2}$) and peak separation (ΔE) were noted from the voltammograms and discussed.

3.8.2 Endosulfan (EDS)

The electrocatalytic behaviour of EDS was investigated using CV in the presence of about 86 μM EDS prepared in 2:1 water/acetonitrile containing 0.1M H_2SO_4 as supporting electrolyte. CV experiments were performed in the potential range -0.8 V to 0.7 V at a scan rate of 25 mVs^{-1}. Comparative electrocatalytic study, stability study and scan rate study of the different

modified electrodes towards EDS reduction was conducted, and different electrochemical parameters discussed.

3.9 Concentration study

3.9.1 Lindane

From the stock solution of 30 nM lindane prepared in 60:40 methanol/water containing 0.05 M TBAB, a series of solutions of 2.2 nM to 18.8 nM were prepared. Current response of varying lindane concentration (2.2 nM to 18.8 nM) was investigated using square wave voltammetry (SWV) at the GCE/AONP/PANI/SWCNT modified electrode. Sensitivity and LoD of the electrodes were calculated from the linear plot of current response versus lindane concentration.

3.9.2 Endosulphan (EDS)

86 μM EDS stock solution was prepared in 2:1 water/acetonitrile containing 0.1 M H_2SO_4 as supporting electrolyte. A series of solutions of 32.3 μM to 77.6 μM were prepared from the stock solution. Electroanalysis was carried out by running SWV in the presence of varying concentrations of EDS at the GCE/AONP/PANI/SWCNT modified electrode. Sensitivity and LoD of the electrodes were calculated from the plot of current response versus EDS concentration.

3.10 Interference Study

3.10.1 Lindane

One millimole solutions of cyclohexane (C_6H_{12}), benzene (C_6H_6), phenol (C_6H_6OH), calcium ions (Ca^{2+}), iron ions (Fe^{2+}), potassium ions (K^+) and magnesium ions (Mg^{2+}) were prepared and their effect on the reduction signal of lindane was investigated. The investigation was carried out by first running cyclic voltammetric experiments with potential range of -1.7 V to -0.2 V at a scan rate of 25 mVs^{-1}, then continuous chronoamperometric (CA) experiments at a potential of 0.2 V. Both experiments were conducted in the presence of various interfering species as well as lindane.

3.10.2 Endosulfan (EDS)

About 1 mM solutions of cyclohexane (C_6H_{12}), benzene (C_6H_6), phenol (C_6H_5OH), lindane ($C_6H_6Cl_6$), chloride ions (Cl^-), Carbonate (CO_3^{2-}), sulphate (SO_4^{2-}) and bicarbonate (HCO_3^-) were prepared and their effect on the reduction signal of EDS was investigated. The investigation was carried out by first running CV in the potential range -0.8 V to 0.7 V at a scan rate of 25 mVs^{-1}, then continuous chronoamperometric (CA) experiments at a potential of 0.2 V. Both experiments were carried out in the presence of various interfering species as well as EDS.

3.11 Real Sample analysis

Real sample analysis was carried out to establish the practical application of the proposed sensor towards Lindane and endosulfan detection in both river water and tap water samples. The river water and tap water were used without further purification and the experiments were repeated three times.

3.11.1 Lindane

Approximately, 7.3 mg lindane was dissolved in 60:40 methanol/river-water containing 0.05 M TBAB to prepare 100 µM (250 mL) lindane stock solution. Lindane samples with concentrations of 50 µM to 0.5 µM were prepared from the stock solution.

About 1.45 mg lindane was dissolved in 60:40 methanol/tap-water containing 0.05 M TBAB to prepare 50 µM (100 mL) lindane stock solution. Lindane samples with concentrations of 40 µM to 10 µM were prepared from the stock solution.

Concentration of the prepared samples was determined by CV in the potential range -1.7 V to -0.2 V at a scan rate of 25 mVs^{-1}.

3.11.2 Endosulfan (EDS)

About 4.07 mg EDS was dissolved in 2:1 river-water/acetonitrile containing 0.1 M H_2SO_4 as supporting electrolyte to prepare 100 µM (100 mL) EDS stock solution. EDS samples with concentrations 80 µM to 20 µM were prepared from the stock solution.

Five hundred milliliter EDS stock solution was prepared by dissolving 50.05 mg EDS in 2:1 tap-water/acetonitrile containing 0.1 M H_2SO_4 as supporting electrolyte. EDS samples with concentrations 146 µM – 46 µM were prepared from the stock solution.

Concentration of the prepared samples was determined by SWV experiments.

CHAPTER 4

RESULTS AND DISCUSSION

4. Results and discussion

4.1 Spectroscopic and Microscopic Characterization

4.1.1 Fourier transform infrared (FT-IR) spectroscopy

Figure 4.1 shows the comparative FT-IR spectra of (a) AONPs, (b) PANI, (c) fSWCNTs and (d) AONP-PANI-SWCNT. From the AONPs spectrum Figure 4.1 (a) the peak observed at 3727 cm^{-1} can be attributed to the stretching and bending vibrations of water. The peak at 733 cm^{-1} can be assigned to the Sb-O-Sb vibrations, whilst the small absorption at 601 cm^{-1} can be attributed to the metal oxygen stretching.[82] The PANI spectrum shows characteristic peaks at approximately 878, 1422, 1575 and 3019 cm^{-1} respectively. The sharp peaks observed at 1575 cm^{-1} and 1422 cm^{-1} are due to the C=N and C=C stretching vibrations of quinoid and benzenoid rings respectively.[83-86] The peak at 878 cm^{-1} can be assigned to the C-H out of plane bending.[83-85] The broad peak at approximately 3019 cm^{-1} can be attributed to by the N-H stretching vibrations.[85] Figure 4.1 (c) depicts FT-IR spectra of acid functionalized single-walled carbon nanotubes and from the spectrum, characteristic peaks are observed at 2930, 2340, 1698, 1104 and 820 cm^{-1}. The two peaks of 2930 cm^{-1} and 2340 cm^{-1} observed in the high frequency region are attributed to the symmetric mode and anti-symmetric mode of CH_2.[87] The peak observed at 1698 cm^{-1} was assigned to the carbonyl strength vibration demonstrating the introduction of a carboxyl group on the surface of the nanotubes.[88] The peak at 1104 cm^{-1} was assigned to either the SWCNT defects or residual carbon impurities or both.[87]

Figure 4.1 (d) depicts the spectrum of the nanocomposite AONP-PANI-SWCNT, the spectrum mostly depicts characteristic of the various nanoparticles used to synthesize the nanocomposite. The peak at 733 cm^{-1} attributed to the Sb-O-Sb stretching vibration confirms the presence of AONPs on the nanocomposite,[82] whilst the C=C stretching vibrations of benzoid rings are presented by the peak at 1422 cm^{-1}. The peak observed at 1698 cm^{-1} was assigned to the carbonyl strength vibration and the two peaks at 2930 cm^{-1} and 2340 cm^{-1} are due to the symmetric and anti-symmetric mode of CH_2.[87]

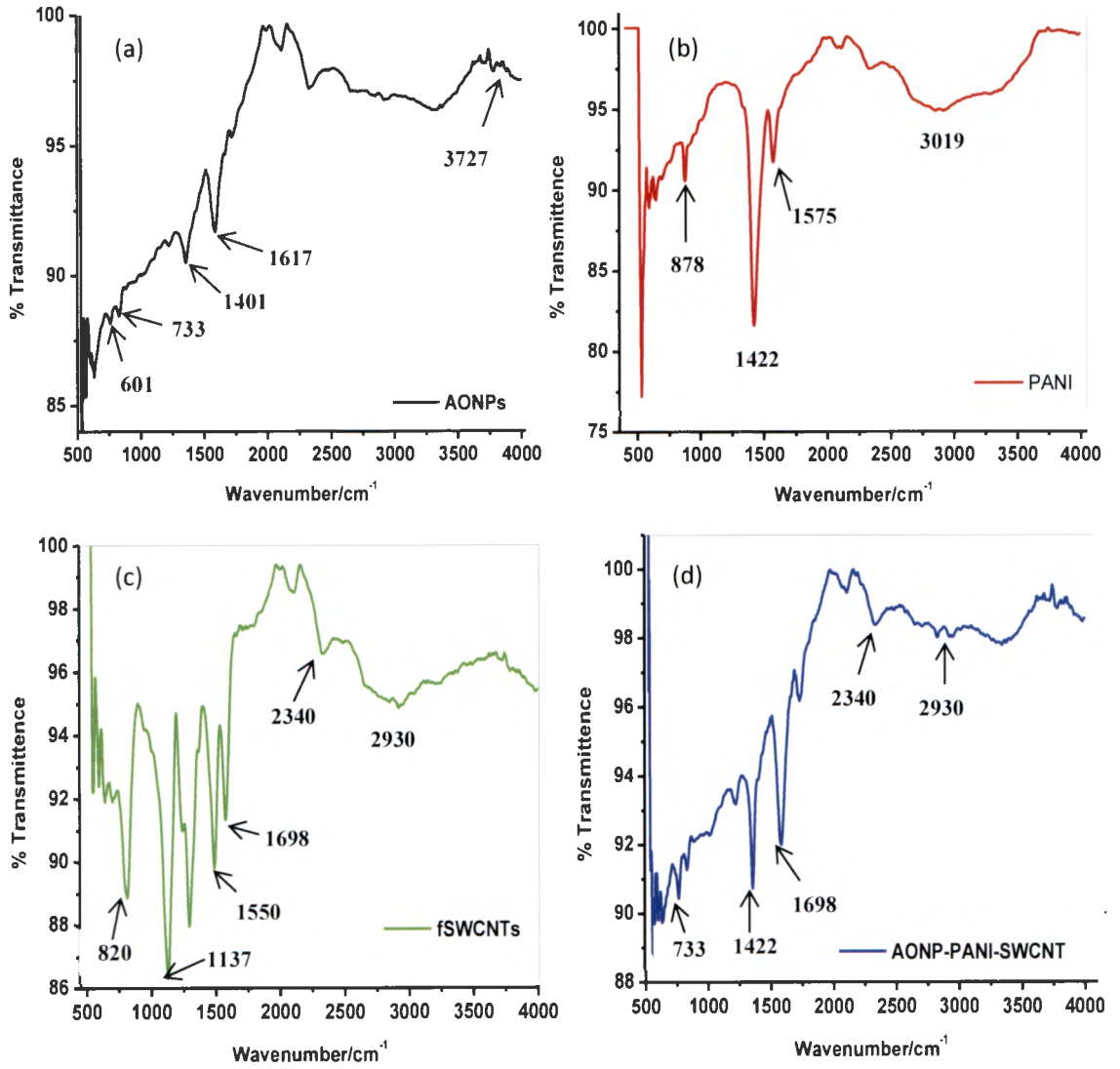

Figure 4.1: FTIR spectra of (a) AONPs, (b) PANI, (c) fSWCNTs and (d) AONP/PANI/SWCNT.

4.1.2 Ultraviolet-visible spectroscopy

Figure 4.2 shows the comparative UV-vis spectra of (a) AONPs, (b) PANI, (c) fSWCNTs and (d) AONP-PANI-SWCNTs. AONPs spectrum shows a sharp peak at about 260 nm which is characteristic of antimony oxide nanoparticles formation.[89] From the spectrum of PANI only two peaks are observed at 341 nm and 650 nm which are assigned to the π-π^* benzenoid transition and the benzenoid to quinoid transition respectively.[62,90] The absorption spectrum of the fSWCNTs showed a significant loss of the van Hove band structure which are typical for

pristine SWCNTs and usually centred around 650 nm and 900 nm.[91-93] Figure 4.2 (d) shows the spectrum of the composite, characteristic peaks of the antimony oxide nanoparticles (AONPs) is observed at around 260 nm which is indicative of the presence of AONPs on the composite.

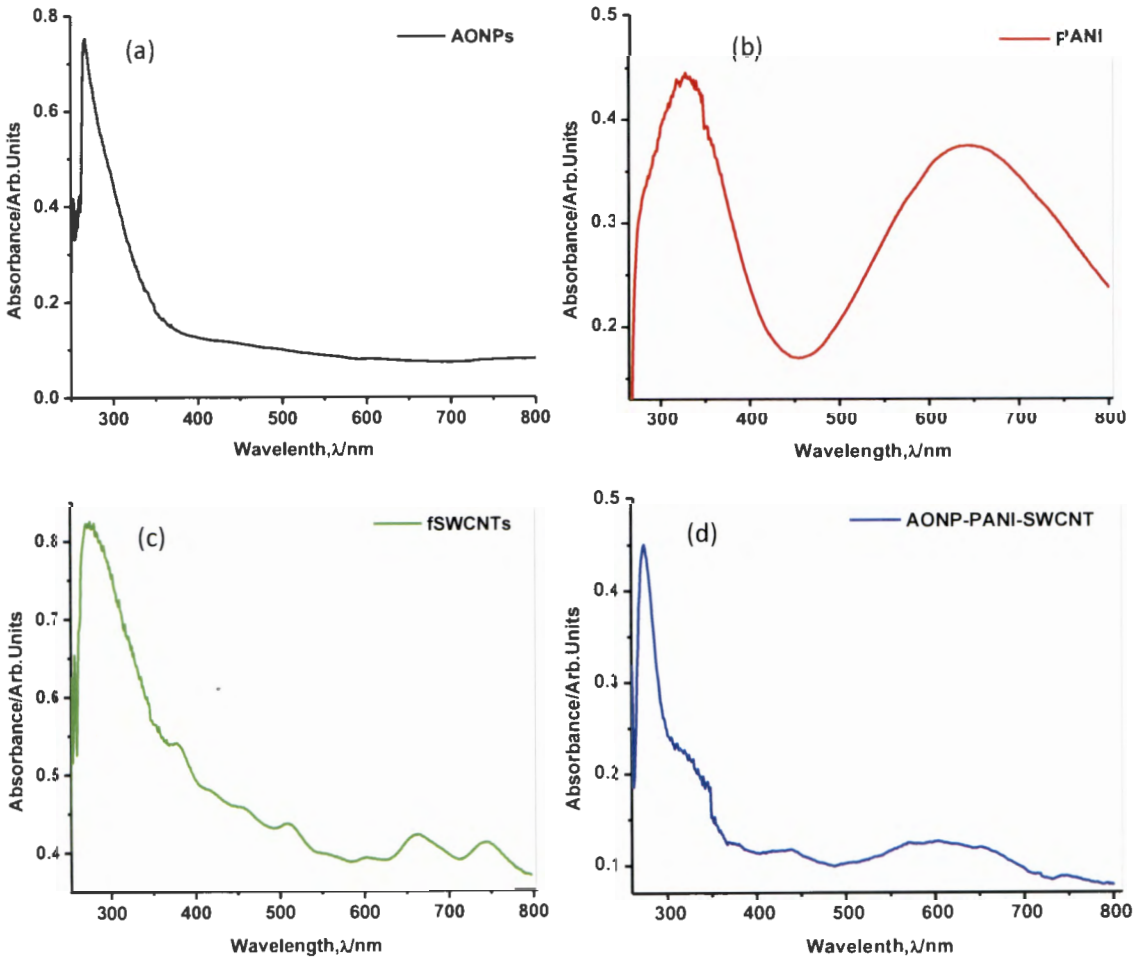

Figure 4.2: UV-vis spectra of (a) AONPs, (b) PANI, (c) fSWCNTs and (d) AONP-PANI-SWCNT.

4.1.3 X-ray diffraction spectroscopy.

Figure 4.3 depicts x-ray diffraction pattern of (a) AONPs, (b) PANI, (c) fSWCNTs and (d) AONP-PANI-SWCNT. Antimony oxide nanoparticles are generally known to exist ir a wide range of compositions and are also known to display interconvertable polymorphism. The two most common forms are cubic and orthorhombic consisting of Sb_4O_6 molecules and chains of

SbO_3 trigonal pyramids.[89] From the AONPs spectra Figure 4.3 (a) a sharp peak is observed at $2\Theta = 37.5°$. From the literature, it was reported that PANI prepared at pH 7 exhibited high crystallinity with the XRD pattern showing an intense peak at $2\Theta = 6.4°$. The peak also indicates that the flower like morphology possesses more ordered conformation which increased solid state ordering. It was further emphasized that crystallinity decreased with a decrease in pH.[62] This confirmed the XRD pattern obtained for PANI (Figure 4.3 (b)) which was synthesized under very acidic conditions. The intensity of the peak at $2\Theta = 6.4°$ is relatively weak. Several sharp peaks observed at $2\Theta = 18.5°$, 19.8°, 23.4°, 25.5°, 26.4°, and 28.4° confirm the high order structure of PANI, however the broad nature of the peaks at 20.4° and 25.5° suggests semi-crystallinity to amorphous nature of the PANI.[62] The peak at $2\Theta = 20.4°$ is assigned to periodicity parallel to the polymer chain and the peak at $2\Theta = 25.5°$ is assigned to periodicity perpendicular to the PANI chains.[62] The XRD spectrum of fSWCNTs is depicted by Figure 4.3 (c) and a broad peak at $2\Theta = 28°$ is observed. The peak is a typical pattern of an amorphous structure.[94]

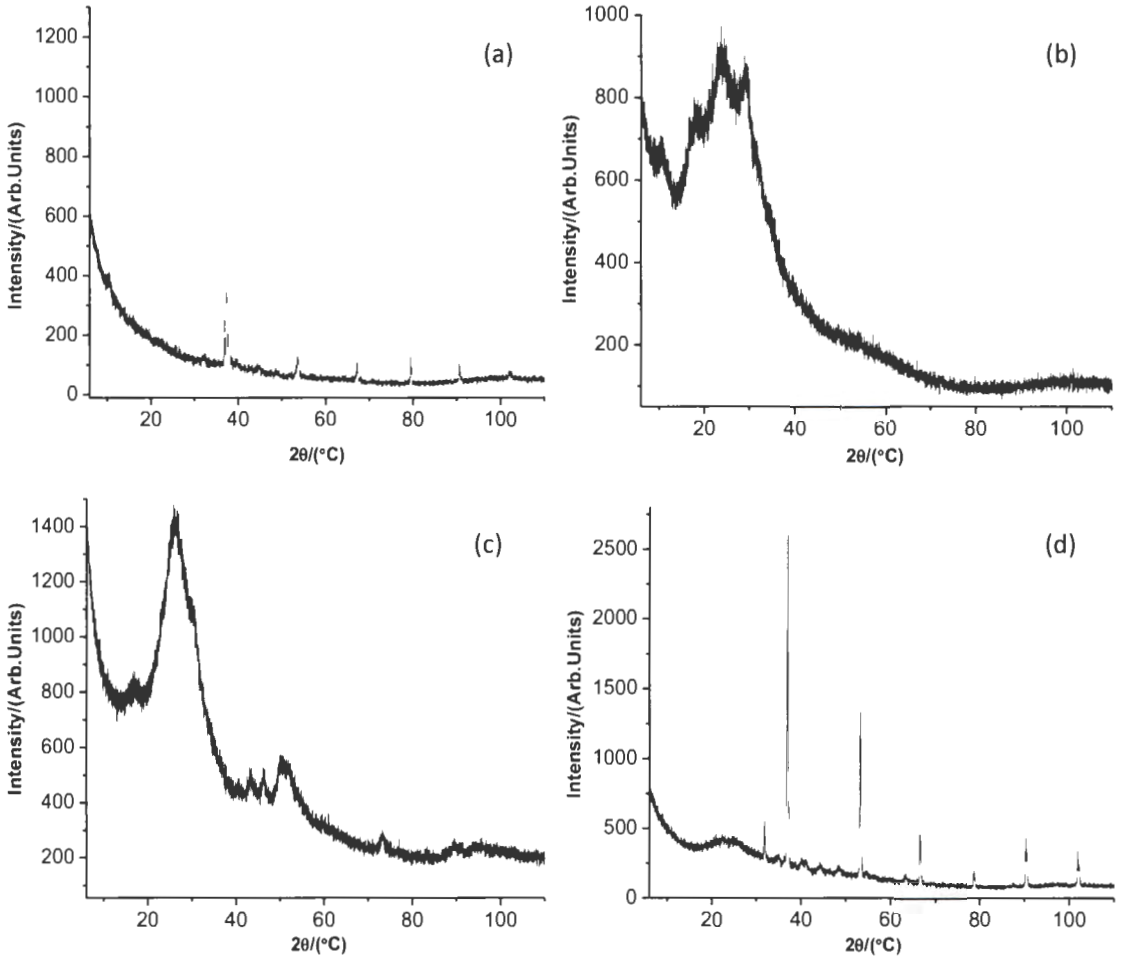

Figure 4.3: XRD spectra of (a) AONPs, (b) PANI, (c) fSWCNTs and (d) AONP-PANI-SWCNT.

4.1.4 Scanning electron microscopy

The morphology of the synthesized nanomaterials was depicted by their respective SEM images, Figure 4.4 shows the SEM images of (a) AONPs, (b) PANI, (c) fSWCNTs and (d) AONP-PANI-SWCNT. The SEM image Figure 4.4 (a) showed that the AONPs appeared unevenly distributed and clustered randomly; the image also depicts compacted flaky platelets. PANI Figure 4.4 (b) showed porous morphology with evenly distributed agglomerations. fSWCNTs Figure 4.4 (c) depicted a large amount of porous tube-like structures that are self-organized in bundles and are unevenly distributed and tangled. The composite AONP-PANI-SWCNT Figure 4.4 (d) shows the characteristics described for antimony oxide nanoparticles

with random clusters but here the clusters are tangled by the SWCNTs resembling a web like formation.

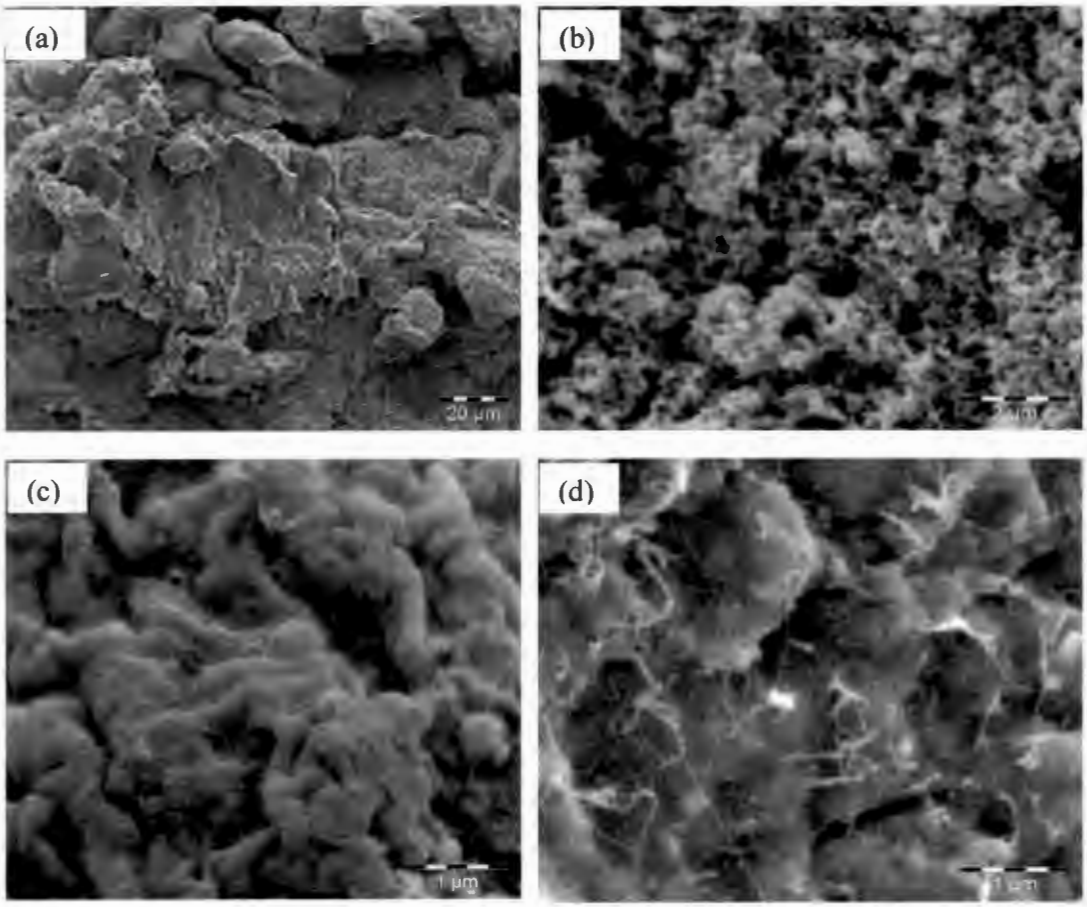

Figure 4.4: SEM images of (a) AONPs, (b) PANI, (c) fSWCNTs and (d) AONP-PANI-SWCNT

4.2 Electrochemical Characterization

4.2.1 Cyclic voltammetric experiments

Cyclic voltammetric studies of the bare and modified GCE were carried out to investigate the electrochemical behavior and electron transport properties of the electrodes. The study was carried out first in 0.1 M PBS (pH 7.0) then in 5 mM $[Fe(CN)_6]^{4-}/[Fe(CN)_6]^{3-}$ solution prepared in 0.1 M PBS both at a scan rate of 25 mVs^{-1}. Figure 4.5 (a) shows the comparative cyclic voltammograms of the modified electrodes in PBS electrolyte. It was observed from the Figure that the electrodes GCE-fSWCNTs and GCE-AONPs-PANI-SWCNT exhibited the highest

current response. SWCNTs are known to enhance the electronic communication between the electrode and the electrolyte solution acting as "Coulombic Islands" (electron transfer stations) and tunnelling electrons between the electrode surface and redox species.[95]

A similar electrochemical behaviour was further observed in the $[Fe(CN)_6]^{4-}/[Fe(CN)_6]^{3-}$ solution. As shown in Figure 4.5 (b), the cyclic voltammetric responses of the electrodes exhibited a pair of well-defined redox peaks characteristic of one-electron transfer redox process in the region 0.0 - 0.4 V typical of $[Fe(CN)_6]^{4-}/[Fe(CN)_6]^{3-}$ redox process.[96] The effective surface area for each electrode was calculated using the Randles-Sevčik equation and calculated as 8.011 x 10^{-4} cm^2, 6.483 x 10^{-4} cm^2, 4.245 x 10^{-4} cm^2, 7.851 x 10^{-5} cm^2 and 1.073 x 10^{-4} cm^2 for GCE-AONP-PANI-SWCNT, GCE-fSWCNTs, GCE-PANI, GCE-AONPs and bare GCE respectively.[97] The observed high current response at the GCE-AONP-PANI-SWCNT associated with fast and ease of electron transfer at the electrode-electrolyte interface is attributed to by the high electroactive surface area of GCE-AONP-PANI-SWCNT.

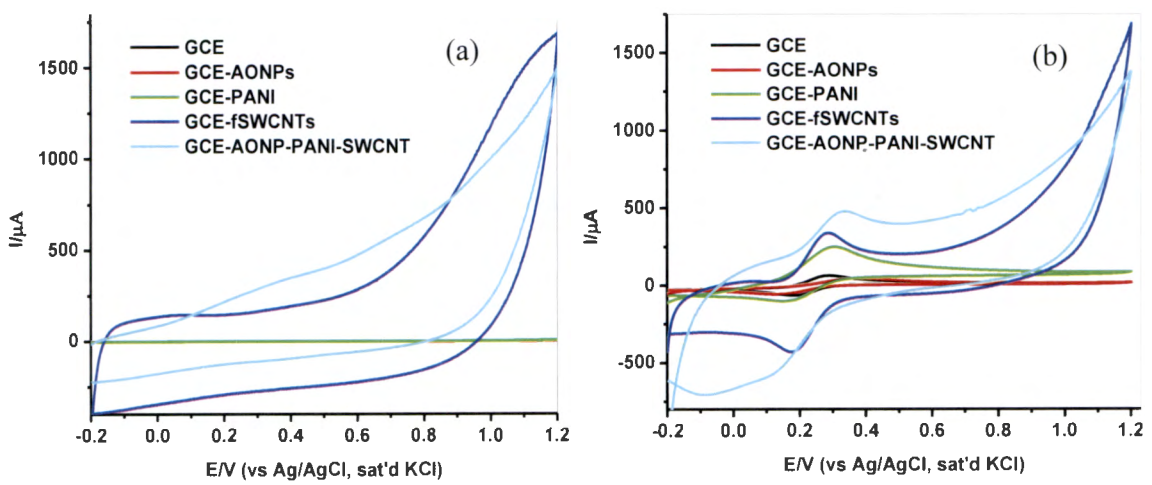

Figure 4.5: Cyclic voltammograms of modified electrodes in (a) 0.1 M PBS solution (b) 5 mM $[Fe(CN)_6]^{4-}/[Fe(CN)_6]^{3-}$ solution prepared in 0.1 M PBS at a scan rate of 25 mVs^{-1}.

Table 4.1 summarizes the electrochemical data and various electrochemical parameters for the electrodes in 5 mM $[Fe(CN)_6]^{4-}/[Fe(CN)_6]^{3-}$ redox probe such as ratio of anodic and cathodic peak current (I_{pa}/I_{pc}), formal potential ($E_{1/2}/V$) and peak separation ($\Delta E_p/V$). I_{pa}/I_{pc} values obtained are closer to 1 indicating that the couple is reversible[98] and the peak-to-peak separation (ΔE_p) values indicate that the electron transport was fastest at the GCE-fSWCNTs electrode (90.3 mV/s) and slowest at the GCE-AONPs electrode (178.3 mV/s). It must be noted that the

overpotential reduced drastically at GCE-AONP-PANI-SWCNT which gave rise to a higher current response recorded at the anode (451 μA) and cathode (499 μA), greater than that of GCE-fSWCNTs (365 μA and 422 μA for the anode and cathode respectively).

Table 4.1: Summary of cyclic voltammetric data obtained for the modified electrodes in 5 mM $[Fe(CN)_6]^{4-/3-}$ prepared in 0.1 M PBS.

Electrode	I_{pa} /μA	I_{pc}/μA	I_{pa}/ I_{pc}	E_{pa}/mV	E_{pc}/mV	ΔEp/mV
GCE	60.4	61.7	0.98	271.1	161.3	109.8
GCE-AONPs	44.2	49.9	0.89	337.1	158.8	178.3
GCE-PANI	239	199	1.20	278.5	161.3	117.2
GCE-fSWCNTs	365	422	0.86	251.6	161.3	90.3
GCE-AONP- PANI-SWCNT	451	499	0.90	278.5	161.3	117.2

4.2.2 Electrochemical impedance spectroscopy

EIS was utilized to investigate the electron transfer properties of the various modified electrodes in $[Fe(CN)_6]^{4-}/[Fe(CN)_6]^{3-}$ solution prepared in 0.1 M PBS. The experiments were conducted at a fixed potential (0.28 V vs Ag/AgCl, sat'd KCl) with a frequency range of 100 kHz – 0.1 Hz. Figure 4.6 depicts the Nyquist plots (a) and Bode plots (b) obtained for the bare-GCE, GCE-AONPs, GCE-PANI, GCE-fSWCNTs and GCE-AONP-PANI-SWCNT electrodes in $[Fe(CN)_6]^{4-}/[Fe(CN)_6]^{3-}$ solution whilst figure 4.6 (c) and (d) depicts the circuit model used to fit the EIS data. Figure 4.6 (c) circuit (R(Q[RW])) was used for bare-GCE, GCE-AONPs and GCE-PANI whilst Figure 4.6 (d) circuit ((RQ)(RC)) was used for GCE-SWCNTs and GCE-AONP-PANI-SWCNT. R_s, R_{ct}, C_{dl}, W and k_s correspond to electrolyte resistance, charge transfer resistance, double layer capacitance, Warburg impedance and electron transfer rate constant respectively.[54],[77] Table 3 summarizes the EIS data obtained for the various modified electrodes. It was observed from the results that GCE-fSWCNT had the lowest R_{ct} value (25.01 Ω cm^2) followed by the composite GCE-AONP-PANI-SWCNT (46.6 Ω cm^2) as compared to that of bare GCE (362 Ω cm^2), GCE-AONPs (274 Ω cm^2) and GCE-PANI (371 Ω cm^2) indicating that modification particularly with the f-SWCNT on the GCE significantly increased the conductivity of the electrode and was more prone to charge transfer.

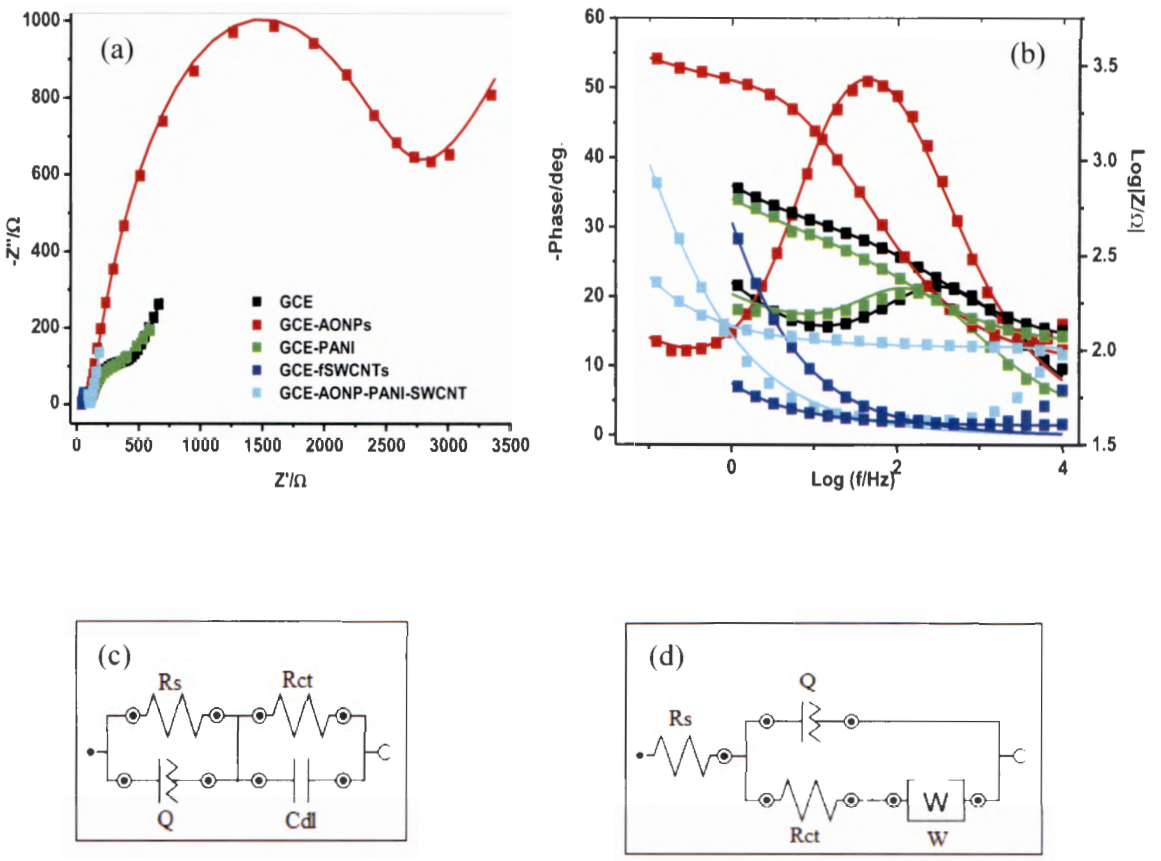

Figure 4.6: (a) Nyquist plots obtained for the modified electrodes in 5 mM $[Fe(CN)_6]^{4-}$/ $[Fe(CN)_6]^{3-}$ solution at a fixed potential of 0.28 V (vs Ag/AgCl, sat'd KCl). The data points are experimental whilst the solid lines represent the non-linear square fits. (b) Bode plots obtained for the modified electrodes in 5 mM $[Fe(CN)_6]^{4-}$/$[Fe(CN)_6]^{3-}$ solution showing the plots of – phase angle/deg. vs log(f/Hz) and log|Z/Ω| vs log(f/Hz). (c) and (d) are the Randle's equivalent circuits used for fitting the EIS data for GCE, GCE-AONPs, GCE-PANI and GCE-fSWCNTs, GCE-AONP-PANI-SWCNT electrodes respectively.

Table 4.2: Summary of the impedance data obtained for the modified electrodes in 5 mM $[Fe(CN)_6]^{4-}$/ $[Fe(CN)_6]^{3-}$ prepared in 0.1 M PBS. The values in brackets represent the percentage errors of the data fitting.

Electrode	R_s (Ω cm^2)	R_{ct} (Ω cm^2)	Q ($x10^{-3}$)	W (Ω cm^2) ($x10^{-3}$)	C_{dl} (nF)	Chisquare ($x10^{-3}$)
GCE	108.3 (0.456)	362 (0.76)	0.0497 (3.508)	1.616 (0.822)	-	2.667
GCE-PANI	106.5 (1.543)	371 (5.138)	0.1103 (11.93)	1.38 4.632	-	34.116
GCE-AONPs	97.5 (1.746)	2740 (2.439)	0.0226 (1.069)	1.344 11.746)	-	123.64
GCE-fSWCNTs	15.87 (0.0)	25.01 (0.934)	7.689 (1.782)	-	125.7 (0.406)	9.5302
GCE-PANI-AONP-SWCNT	60.7 (7.85)	46.6 (9.563)	7.79 (1.181)	-	271.6 (0.521)	32.658

4.3 Electrocatalytic studies of lindane

4.3.1 Electrocatalytic reduction of lindane

The electrochemical behaviour of lindane was investigated using CV in the presence of 9 µM lindane prepared in 60:40 methanol/water containing 0.05 M TBAB. The potential window of -0.2 to -1.7 V with reference to Ag/AgCl satd'd KCl and scan rate of 25 mVs^{-1} were the experimental conditions. Figure 4.7 (a) shows the comparative cyclic voltammograms obtained for GCE, GCE-AONPs, GCE-PANI, GCE-fSWCNTs and GCE-AONP-PANI-SWCNT in the presence of 9 µM lindane. The obtained reduction peaks with no anodic peaks suggests that the electrocatalysis of lindane is an irreversible reaction and similar results have been reported.[39,68,99,100] From the voltammogram in Figure 4.7 (a) the reduction peak was observed at -1.14 V for bare GCE, -0.57 V for GCE-AONPs, -0.50 V for GCE-PANI, -0.9 V for GCE-fSWCNT and -0.95 V for GCE-AONP-PANI-SWCNT. Generally the modified electrodes shifted to a more positive potential as compared to that of the bare GCE. Furthermore, the

measured reduction currents are 43.5 μA, 9.39 μA, 16 μA, 169 μA and 267 μA for bare GCE, GCE-AONPs, GCE-PANI, GCE-fSWCNTs and GCE-AONP-PANI-SWCNT respectively. It was interesting to note that unlike in the electrochemical characterization figure 4.5 (b) the reduction current for bare GCE was higher than that of GCE-PANI and GCE-AONPs by at least 2 folds, while the reduction current for GCE-AONP-PANI-SWCNT significantly increased by over six folds as compared to that of bare GCE. This may be due to the high electrocatalytic activity and strong adsorption capabilities of the nanomaterial on the modified electrodes.[27]

The GCE-AONP-PANI-SWCNT modified electrode proved superior to the other electrodes and thus its stability and resistance towards lindane reduction product fouling effect was further explored by CV for 20 scans. Figure 4.7 (b) depicts twenty cyclic scans of GCE-AONP-PANI-SWCNT modified electrode in the presence of 9 μM lindane prepared in 60:40 methanol/water containing 0.05 M TBAB 20 scans at a scan rate of 25 mVs^{-1} with the same experimental conditions as above. Lindane reduction current was stable with virtually no current decrease between the 1st and 20th scan as depicted by figure 4.7 (b), thus the GCE-AONP-PANI-SWCNT electrode demonstrated good stability to electrode fouling effect.

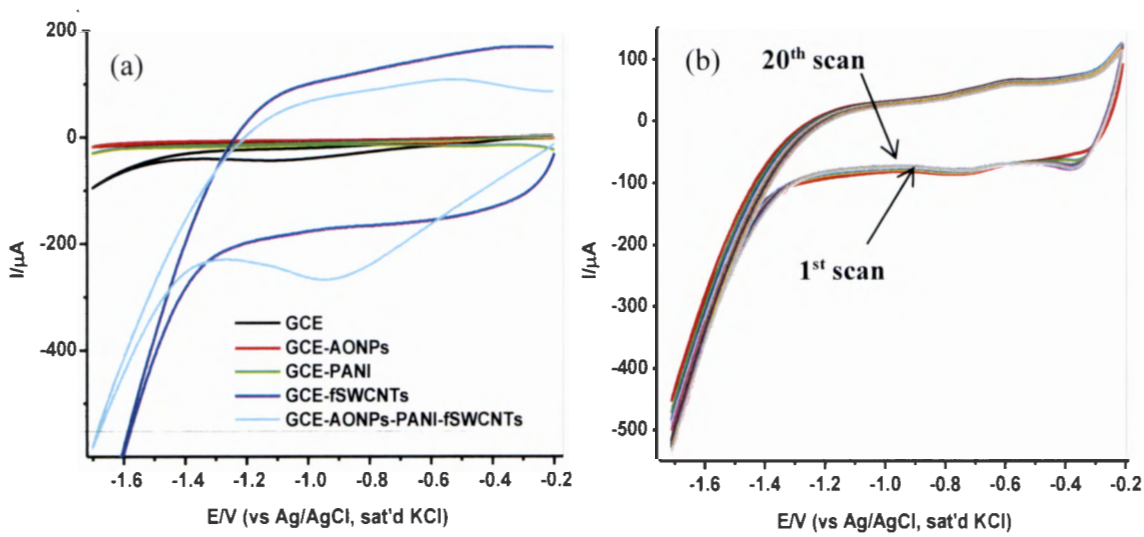

Figure 4.7: (a) Cyclic voltammograms of the GCE modified electrodes in the presence of 9 μM lindane prepared in 60:40 methanol/water containing 0.05 M TBAB at a scan rate of 25 mVs^{-1}. (b) Cyclic voltammograms (20 scans) of GCE-AONP-PANI-SWCNT modified electrode in the presence of 9 μM lindane prepared in 60:40 methanol/water containing 0.05 M TBAB at a scan rate of 25 mVs^{-1}.

4.3.2 Effect of scan rate on lindane reduction

Effect of scan rate (range 25 – 1000 mVs^{-1}) was investigated by conducting CV experiments in the presence of 9 µM lindane prepared in 60:40 methanol/water containing 0.05 M TBAB using GCE-AONP-PANI-SWCNT modified electrode. The potential window of -0.2 to -1.7 V with reference to Ag/AgCl satd'd KCl were the experimental conditions chosen. Figure 4.8 (a) depicts the cyclic voltammograms obtained and it was observed that the lindane reduction peak current increased simultaneously with increasing scan rate suggesting diffusion controlled process.[97,100-101] Figure 4.8 (b) shows the plot of anodic peak current (I_{pa}) against square root of scan rate ($v^{1/2}$) with a linear regression of $I = -1.4147v^{1/2} + 1.4058$ and a correlation coefficient of $R^2 = 0.9851$. The non-zero intercept can be attributed to an adsorption process after diffusion.[67] It was proposed that the mechanism of lindane reduction proceeds via a dissociative electron transfer (DET) mechanism leading to the scission of the carbon-chlorine bond. The mechanism may occur either in a step-wise mechanism with the formation of an intermediate radical and an anion as shown by scheme 4.1, or in a concerted mechanism yielding directly a radical and an anion shown by scheme 4.2.[99,100]

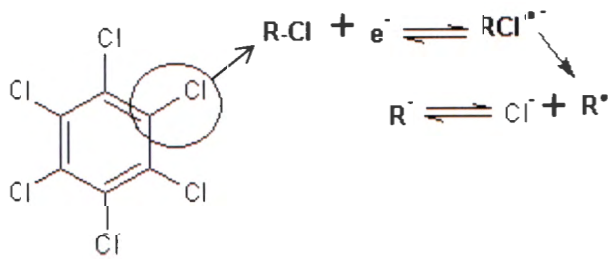

Scheme 4.1: Stepwise mechanism of lindane reduction[99,100]

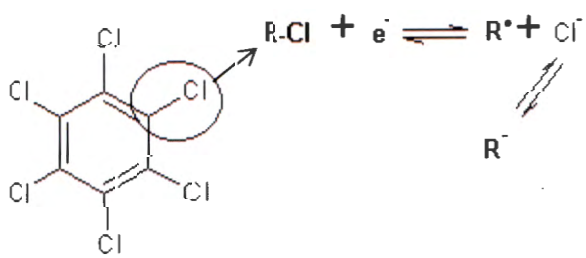

Scheme 4.2: Concerted mechanism of lindane reduction[99,100]

Furthermore it was reported that the methanol-water medium was favourable for the reduction of lindane to benzene, were water acts as a proton donor to the electrogenerated carbanion intermediate which then undergoes a six electron reduction to yield benzene.[99]

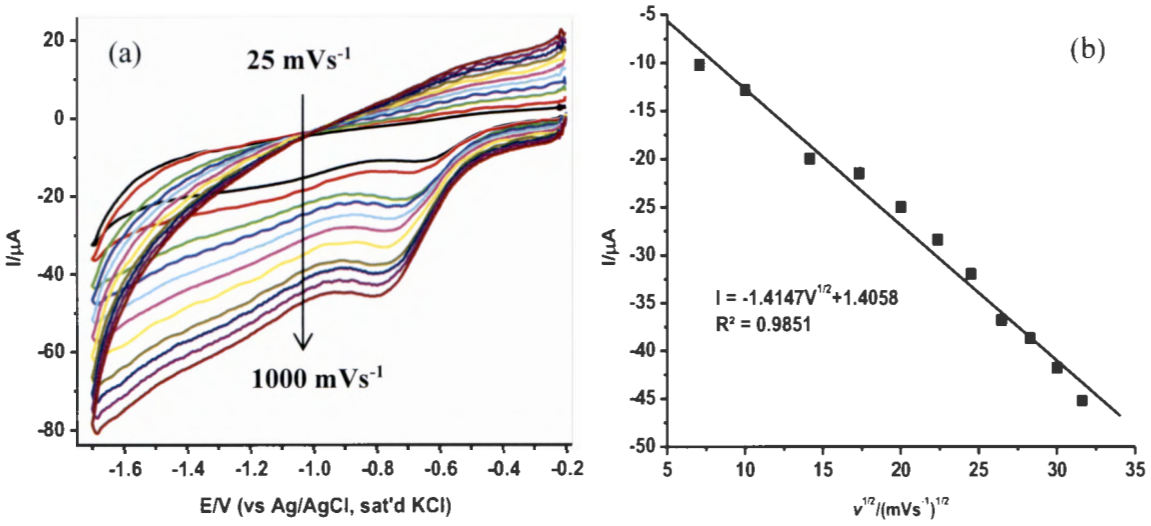

Figure 4.8: (a) Cyclic voltammograms of GCE-AONP-PANI-SWCNT modified electrode in the presence of 9 μM lindane prepared in 60:40 methanol/water containing 0.05 M TBAB at a scan rate of 25 – 1000 mVs^{-1}. (b) Plot of anodic peak current (I_{pa}) against square root of scan rate (v) for GCE-AONP-PANI-SWCNT modified electrode.

4.3.3 Electroanalysis of lindane

The effect of current response on varying lindane concentration (0 to 18.8 nM) was carried out using SWV so as to improve the sensitivity of the proposed method. SWV experiments were carried out in various concentrations of lindane in the presence of 60:40 methanol/water containing 0.05 M TBAB. Figure 4.9 (a) depicts square-wave voltammograms obtained for the GCE-AONP-PANI-SWCNT modified electrode with varying concentrations of lindane, (b) depicts plot of current response versus lindane concentration with a linear regression of I_p = 202.5[lindane] + 80.997 and correlation coefficient of R^2 = 0.9903. It was observed from figure 18(a) that the lindane reduction peak current simultaneously increased with the increase in lindane concentration and the potential gradually shifted negatively with increasing lindane concentration. On Figure 4.9 (b) the linear response obtained was satisfactory over the range of lindane concentrations 0.0 to 18.8 nM with a linear regression of I_p = 202.5[lindane] +

80.997 and correlation coefficient of $R^2 = 0.9903$. The limit of detection (LoD) was calculated using equation 4.1,

$$LoD = 3.3\,{}^{\delta}/_{m} \qquad 4.1.$$

Where δ is the relative standard deviation of the intercept of the y-coordinates from the line of best fit on the linear current versus lindane concentration; m is the slope of the same line.[104] The LoD, limit of quantification (LoQ) and sensitivity of the GCE-AONP-PANI-SWCNT electrode toward lindane was determined to be 2.01 nM, 6.09 nM and 202.5 μA/μM respectively. The LoD and sensitivity (2.01 nM, 202.5 μA μM^{-1}) reported here was found to be better than those reported at $NiCo_2O_4$ modified GCE (3.6 μM, 0.2 μA/μM),[16] cellulose acetate modified GCE (37 μM),[100] Nylon6,6/MWCNT/Fe_3O_4 modified GCE (32 nM)[39] and CuO/MnO_2 hierarchical nano-microstructures (4.8 nM, 0.022 μA/μM).[67] This suggests that the AONP-PANI-SWCNT modified GCE has good electrocatalytic activity for the electro-oxidation of lindane table 4 summarizes the comparison of analytical performance of AONP-PANI-SWCNT modified GCE electrode with other non-enzymatic sensors reported for electrocatalytic detection of lindane.

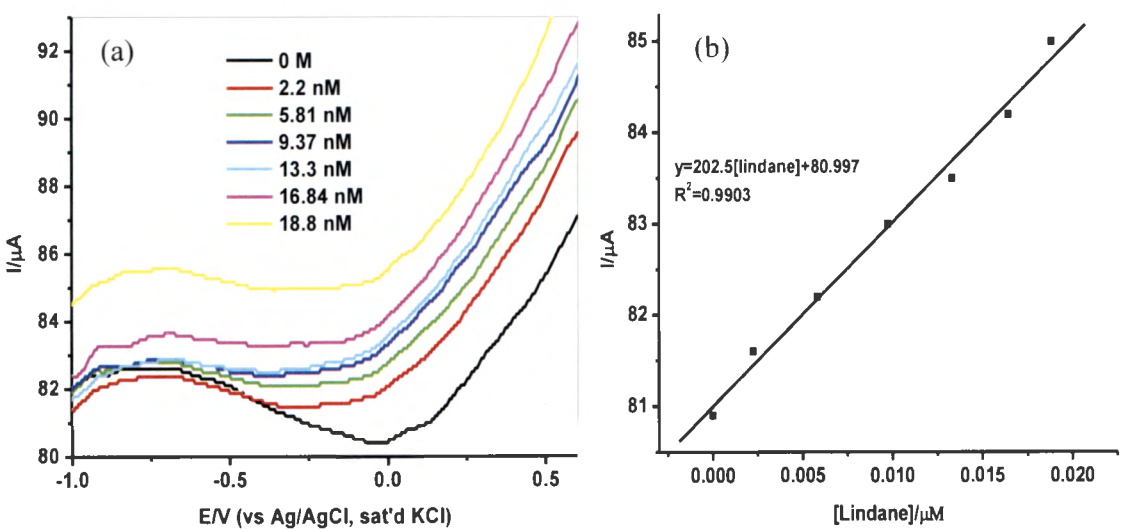

Figure 4.9: (a) Square-wave voltammograms of GCE-AONP-PANI-SWCNT modified electrode in 0.0 nM to 5.19 nM lindane prepared in 60:40 methanol/water containing 0.05 M TBAB. (b) Plot of current response versus lindane concentration.

Table 4.3: Comparison of analytical performance of AONP-PANI-SWCNT modified GCE electrode with other non-enzymatic sensors reported for electrocatalytic detection of lindane.

Composite electrode	LoD	Linear range	Sensitivity	Reference
$NiCo_2O_4$/GCE	**3.6 µM**	**10 µM -170 µM**	**0.2 µA/µM**	**[16]**
CA /GCE	37 µM	50 µM – 1000 µM	-	[100]
Nylon6,6/MWCNT/Fe_3O_4/GCE	**32 nM**	**9.9 pM – 5.0 µM**	**-**	**[39]**
CuO/MnO_2/GCE	4.8 nM	0.0 µM – 700 µM	0.022 µA/µM	[68]
αMnO_2-NW/GCE	**114 nM**	**1.1 µM – 510 µM**		**[38]**
AgNPs(5%)-PANI-Nano-ZSM-5/GCE	5 nM	0.01 µM – 0.9 mM	1.24 mA/µM	[99]
GCE-AONP-PANI-SWCNT	**2.01 nM**	**0.0 nM - 18.8 nM**	**202.5 µA/µM**	**Present study**

Abbreviations: GCE – Glassy carbon electrode, CA – Cellulose acetate, MWCNT – Multi-walled carbon nanotube, NW – Nanowires, Nano-ZSM-5 – Nanocrystalline Zeolite Socony Mobil-5, PANI – Polyaniline.

4.3.4 Lindane interference studies

Interference studies were carried out to investigate the selectivity of the developed sensor towards lindane determination using cyclic voltammetry (CV) and continuous chronoamperometry (CA) methods. The selection of interfering species chosen for this study was based on either structural similarity and solubility in water and soil, as well as the fact that these species may be present in water or soil from industrial areas and agricultural land given the historical use of lindane both in industry and agriculture.[38,39,100] The chosen species which may potentially interfere with lindane determination included electroactive organic compounds such as cyclohexane (C_6H_{12}), benzene (C_6H_6), phenol (C_6H_5OH) and some inorganic cations which included calcium (Ca^{2+}), potassium (K^+), magnesium (Mg^{2+}), and iron (Fe^{2+}). Figure 4.10 (a) shows continuous chronoamperometric response at the GCE-AONP-PANI-SWCNT modified electrode respectively with addition of 1 mM each of lindane, C_6H_{12}, C_6H_6, C_6H_5OH, then lindane and the inorganic cations Ca^{2+}, K^+, Mg^{2+}, Fe^{2+} followed by three successive additions of lindane in the presence of 60:40 methanol/water containing 0.05 M TBAB at a fixed potential of 0.2 V. The results indicated that the GCE-AONP-PANI-SWCNT modified electrode can be used for selective determination of lindane in the two media (organic and inorganic). The addition of lindane to the water sample shows a more positive current peak but

after the addition of organic compounds such as C_6H_{12}, C_6H_6 and C_6H_5OH the response intensity was shifted to a less positive current peak which indicate reduction. Addition of phenol shows further hydroxylation by the hydroxyl ions in the reaction mixture and confirms removal of chloride from chlorobenzene was not feasible through reduction process but it was achieved through substitution reaction, whereas the formation of catechol advocated that hydrodechlorination process occurred in first phase prior to that of second phase was not affected by the interfering species suggesting that the electrode is highly selective towards lindane detecion.

Figure 4.10 (b) shows the variation of reduction signal for interfering species with respect to lindane as a percentage at GCE-AONP-PANI-SWCNT modified electrode in 0.05 M TBAB 60:40 methanol/water (at a scan rate of 25 mVs^{-1}) using cyclic voltammetry technique. CV results obtained showed that the GCE/AONP/PANI/SWCNT modified electrode had anti-interference behaviour towards the detection of lindane in the presence of interfering species with an average of only 12.1 % current drop on the CV reduction signal of lindane.

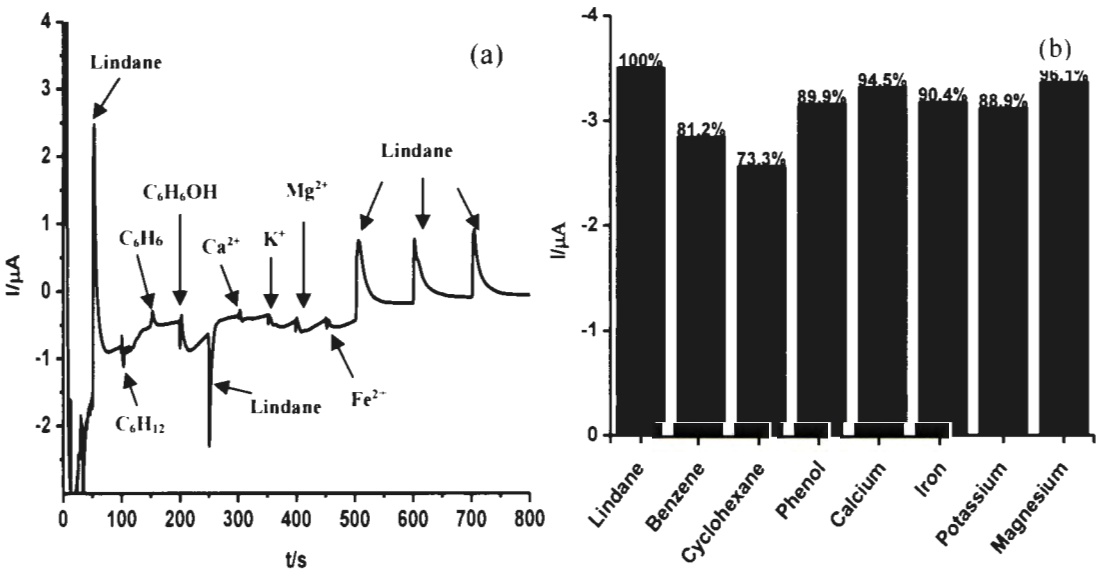

Figure 4.10: (a) Continuous chronoamperometric response of 1 mM lindane at GCE/AONP/PANI/SWCNT modified electrode in the presence of 1 mM interfering species such as cyclohexane, benzene, phenol, Ca^{2+}, K^+, Mg^{2+} and Fe^{2+} ions. (b) Variation of reduction signal for interfering species with respect to lindane as a percentage at GCE/AONP/PANI/SWCNT modified electrode in 0.05 M TBAB 60:40 methanol/water at a scan rate of 25 mVs^{-1} using cyclic voltammetry technique.

4.3.5 Lindane real sample analysis

Real sample analysis was carried out to establish the practical application of the GCE/AONP/PANI/SWCNT modified electrode towards lindane detection in both river water and tap water samples. The river water samples were collected from upper crocodile sub – catchment of Crocodile River in Rustenburg of the North West province, South Africa. This river water system is known to receive runoff from agricultural land as well as effluents from the industrial mines around the area. The samples were collected from a point in the river with GPS coordinates: S 025° 40` 09.3 E 027° 47` 31.7 and labeled A. The river water was used without further purification. Lindane samples with concentrations ranging from 0.5 µM – 100 µM were prepared by using 60:40 methanol/river-water containing 0.05 M TBAB. CV studies were conducted to determine the concentration of lindane in the samples; results obtained are presented in Table 5. It was observed that recoveries of lindane at lower concentrations of lindane was at an average of 180 % suggesting the presence of lindane in the river water samples, however at higher concentrations, this was not the case as the average recovery was only 97.1%, this may be due to the sensor`s linear range.

Tap water was collected from a residential area Lomanyaneng village, Mahikeng in the North West province of South Africa with GPS coordinates S 25° 54. 251` E 025° 38.412`. The water was supplied by the local municipality and was used without further purification. Lindane samples with concentrations ranging from 10 µM – 50 µM were prepared by using 60:40 methanol/tap-water containing 0.05 M TBAB. The sensor yielded good recoveries (99.9 % average) at lower concentrations of lindane when compared to higher concentrations (86.5 % average) with an overall average of 93.2 %.

Table 4.4: Determination of Lindane concentration in river water and tap water samples using CV method.

Sample	Compound	Added (μM)	Found[a] (μM)	Recovery (%)	RSD (%)
River water	Lindane	0.5	1.0	200	14.4
		1	1.6	160	10.1
		20	18.7	94	12.9
		100	100.2	100.2	0.35
Tap Water	Lindane	10	9.87	98.7	3.51
		20	20.3	101	2.99
		40	33.6	84	3.88
		50	44.3	89	4.01

[a]Average value of three determinations

4.4 Electrocatalytic studies of endosulfan

4.4.1 Electrocatalytic reduction of endosulfan (EDS)

The electrochemical behaviour of EDS was investigated using CV in the presence of 86 μM EDS prepared in 2:1 water/acetonitrile containing 0.1M H_2SO_4. The potential window of -0.8 to 0.5 V with reference to Ag/AgCl satd'd KCl and scan rate of 25 mVs^{-1} were the experimental conditions. Figure 4.11 (a) shows the comparative cyclic voltammograms obtained for GCE, GCE-AONPs, GCE-PANI, GCE-fSWCNTs and GCE-AONP-PANI-SWCNT electrode in the presence of 86 μM EDS. Well-defined irreversible reduction peaks were obtained at -0.45 V, -0.37 V, -0.31 V, -0.27 V and 0.13 V for bare GCE, GCE-AONPs, GCE-PANI, GCE-fSWCNTs and GCE-AONP-PANI-SWCNT respectively with corresponding reduction currents of -5.52 μA, -0.168 μA, -11.4 μA, -59 μA and -510 μA. The highest reduction current was recorded at the GCE-AONP-PANI-SWCNT modified electrode.

GCE-AONP-PANI-SWCNT modified electrode proved superior to the other electrodes and thus its stability and resistance towards EDS reduction product was further explored using CV by running 20 scans in the analyte. Figure 4.11 (b) depicts cyclic voltammograms (20 scans)

at GCE-AONP-PANI-SWCNT modified electrode in the presence of 86 μM EDS prepared in 2:1 water/acetonitrile containing 0.1M H_2SO_4 at a scan rate of 25 mVs^{-1} and potential window of -0.8 to 0.5 V with reference to Ag/AgCl satd'd KCl. EDS reduction current was stable with virtually no current drop between the 1st and 20th scan as depicted by Figure 4.11 (b), thus the GCE-AONP-PANI-SWCNT electrode demonstrated good stability to electrode fouling effect.

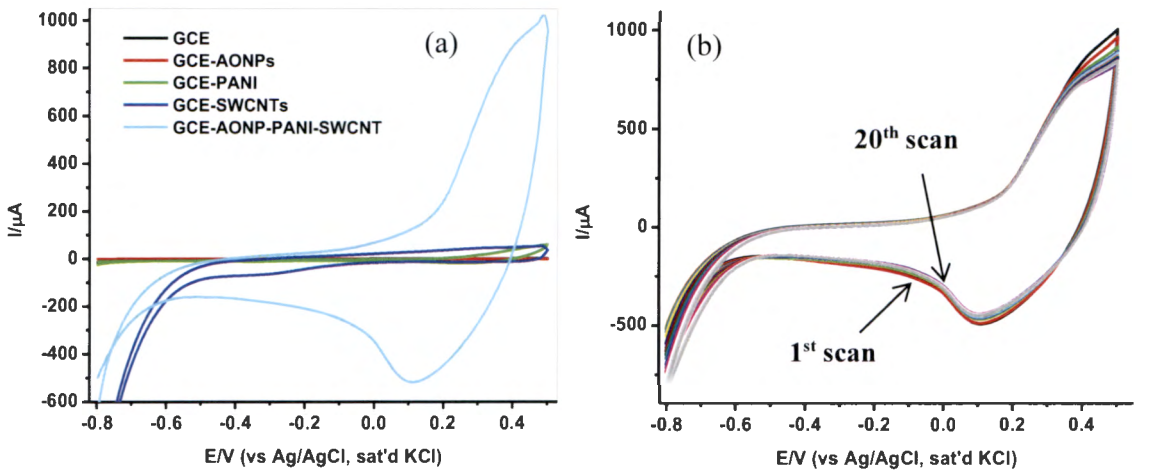

Figure 4.11: (a) Cyclic voltammograms of modified electrodes in the presence of 86 μM EDS prepared in 2:1 water/acetonitrile containing 0.1 M H_2SO_4 at a scan rate of 25 mVs^{-1}. (b) Cyclic voltammograms of GCE-AONP-PANI-SWCNT modified electrode in the presence of 86 μM EDS prepared in 2:1 water/acetonitrile containing 0.1 M H_2SO_4 20 scans at a scan rate of 25 mVs^{-1}.

4.4.2 Effect of scan rate on endosulfan reduction

Effect of scan rate (range 25 – 1000 mVs^{-1}) was investigated by conducting CV experiments in the presence of 86 μM EDS prepared in in 2:1 water/acetonitrile containing 0.1 M H_2SO_4 using GCE-AONP-PANI-SWCNT modified electrode. The potential window of -0.8 to 0.5 V with reference to Ag/AgCl satd'd KCl were the experimental conditions. Figure 4.12 (a) depicts the cyclic voltammograms obtained and it is observed that the EDS reduction peak current increased simultaneously with the increase of scan rate suggesting diffusion controlled process.[96,100-101] Figure 4.12 (b) shows the Plot of anodic peak current (I_{pa}) against square root of scan rate ($v^{1/2}$) with a linear regression of $I = -35.38v^{1/2} - 686.56$ and correlation coefficient of $R^2 = 0.9881$. It was reported in literature that EDS cannot dissociate due to its molecular

structure,[105] it was further reported that EDS has no oxidizing properties, has no acid proton or a reasonable amount of basic centres. However EDS is said to be sensitive to acids, alkalis and moisture, its electrochemical reduction is thereby heavily dependent on the cell constituents, supporting electrolyte and potential window.[105,106] EDS structure has numerous chlorine atoms located at different positions, thus it is prone to reduction at these carbon-chlorine positions. However literature reports suggested that there is a transition state for electron transfer in the carbon-chlorine bond that is orientated perpendicular to the electrode surface with the chlorine atom nearest to the electrode. It was further established that EDS reduction occurs at the C(7)-Cl(13) bond and the argument has been that the structure resulting from this bond rupture is the most stable, this was supported by the evaluation of the lowest unoccupied molecular orbital (LUMO) of EDS. From the above it was deduced that the most feasible mechanism of EDS reduction in acidic medium involved two steps. On the first step a radical is formed due to the reduction of the chlorine atom connected to the carbon in C(7) position, this involves only one electron. The radical is reduced on the second step involving one more electron and proton, this proposed mechanism is shown by scheme 4.3. [107]

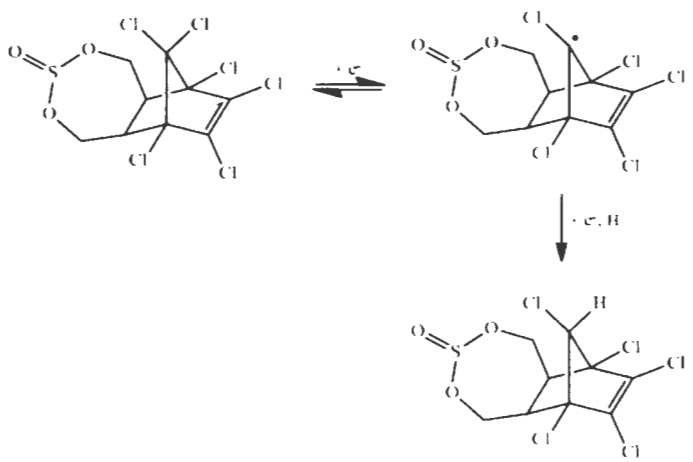

Scheme 4.3: EDS reduction mechanism[107]

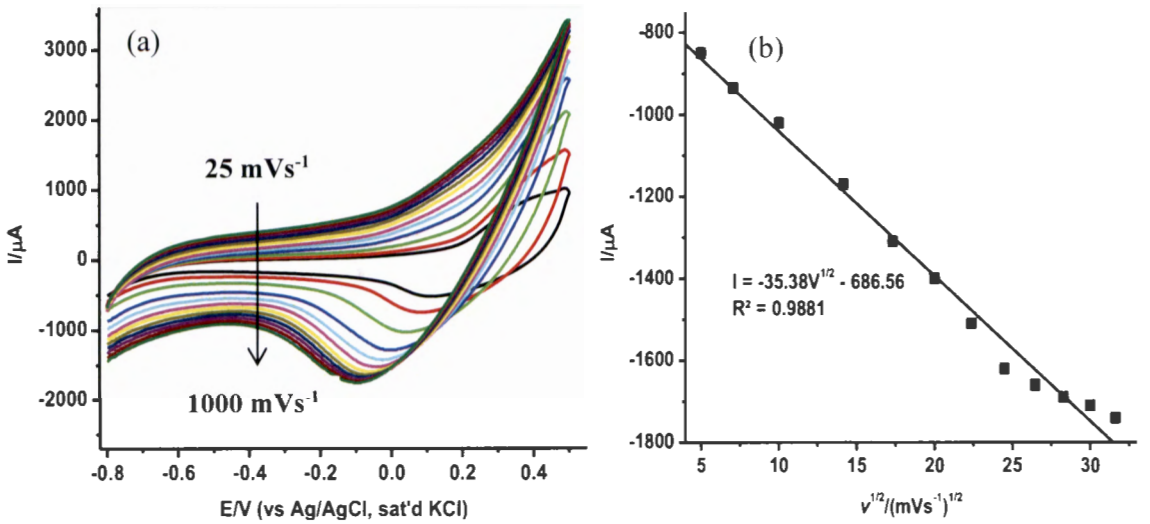

Figure 4.12: (a) Cyclic voltammograms of GCE-Sb_2O_3-PANI-SWCNT modified electrode in the presence of 86 µM EDS prepared in 2:1 water/acetonitrile containing 0.1M H_2SO_4 at a scan rate of 25 – 1000 mVs^{-1}. (b) Plot of anodic peak current (I_{pa}) against square root of scan rate (v) for GCE-AONP-PANI-SWCNT modified electrode.

4.4.3 Electroanalysis of Endosulfan

The effect of current response on varying EDS concentration (32.3 to 77.6 µM) was carried out using square wave voltammetry (SWV). SWV experiments were carried out in various concentrations of EDS prepared in 2:1 water/acetonitrile containing 0.1 M H_2SO_4. Figure 4.13 (a) depicts square-wave voltammograms obtained for the GCE-AONP-PANI-SWCNT modified electrode with varying concentrations of EDS. Figure 4.13 (b) depicts plot of current response versus EDS concentration with a linear regression of I = -0.2086[EDS] + 2.8497 and correlation coefficient of R^2 = 0.9952. It was observed from Figure 4.13 (a) that the EDS reduction peak current simultaneously increased with increase in EDS concentration. While the potential gradually shifted negatively with increasing EDS concentration.

The LoD, LoQ and sensitivity of the GCE-AONP-PANI-SWCNT electrode toward EDS was determined to be 5.22 µM, 15.8 µM and 0.2086 µA/µM respectively. The LoD value for EDS reported here (5.22 µM) was found to be lower as compared to that reported at Molecular imprinted polymer (MIP) (20 µM),[108] but higher than that reported at hanging mercury drop electrode (HMDE) (0.297 µM).[107] The AONP-PANI-SWCNT modified GCE demonstrated

good electrocatalytic activity for the electro-reduction of EDS and the results obtained (Table 4.5) are comparable to other reported methods. It must be admitted that literature on electrochemical detection of EDS was very scarce and therefore signifying the novelty of this study especially using AONP-PANI-SWCNT composite modified GCE. Table 4.5 summarizes the analytical performance of AONP-PANI-SWCNT modified GCE compare with other sensors reported for EDS detection.

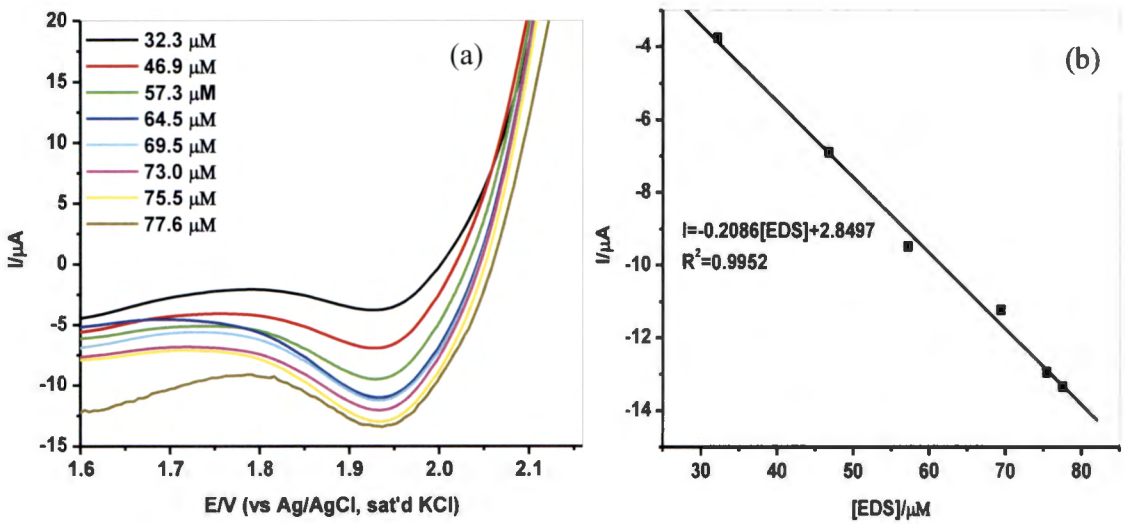

Figure 4.13: (a) Square wave voltammograms of GCE-AONP-PANI-SWCNT modified electrode in 32.3 µM to 77.6 µM EDS prepared prepared in 2:1 water/acetonitrile containing 0.1 M H_2SO_4. (b) Plot of current response versus EDS concentration.

Table 4.5: Comparison of analytical performance of AONP-PANI-SWCNT modified GCE electrode with other sensors reported for electrocatalytic detection of EDS.

Composite electrode	LoD	Linear range	Sensitivity	Reference
MIP	0.02 mM	0.02 mM -0.12 mM	-	[108]
HMDE	0.297 µM	0.154 µM – 0.157 µM	0.0188 µA μM^{-1}	[107]
GCE-AONPs-PANI-SWCNT	5.22 µM	32.3 µM – 77.6 µM	0.2086 µA μM^{-1}	Present study

Abbreviations: MIP – Molecularly imprinted polymer, HMDE – Hanging mercury drop electrode.

4.4.4 Endosulfan interference studies

Interference studies were carried out to investigate the selectivity of the developed sensor towards EDS determination by CV and CA. Possible interfering species selected for the study included some electroactive organic compunds such as cyclohexane (C_6H_{12}), benzene (C_6H_6), phenol (C_6H_5OH), organochlorine pesticide lindane ($C_6H_6Cl_6$) and various anions such as chloride (Cl^-), Carbonate (CO_3^{2-}), sulphate (SO_4^{2-}), and bicarbonate (HCO_3^-). These were selected based on either structural similarity, solubility in water and soil as well as the fact that these species may be present in water or soil from industrial areas and agricultural land. Figure 4.14 (a) shows continuous chronoamperometric response at the GCE-AONP-PANI-SWCNT modified electrode with addition of 1 mM each of EDS, cyclohexane, benzene, phenol, lindane; and the inorganic anions Cl^-, CO_3^{2-}, SO_4^{2-}, and HCO_3^- followed by three successive additions of EDS in the presence of 2:1 water/acetonitrile containing 0.1 M H_2SO_4 and a fixed potential of 0.2 V. The results obtained showed that the presence of EDS had no influence on the signal response for cyclohexane, benzene, phenol, lindane; and the inorganic anions Cl^-, CO_3^{2-} and SO_4^{2-}. The orientation of the signal changes towards a less negative current response after the addition of the anion HCO_3^- this also further influences the orientation of the EDS detection signal by shifting to a less negative current. This further confirms that the modified electrode can be used for selective determination of EDS in the presence of cations and anions commonly found in water or soil samples.

Selectivity of the sensor is further demonstrated by Figure 4.14 (b) which shows the variation of reduction signal for interfering species with respect to EDS as a percentage using cyclic voltammetry at GCE-AONP-PANI-SWCNT modified electrode in 2:1 water/acetonitrile containing 0.1 M H_2SO_4 at scan rate of 25 mVs^{-1}. The results indicate that the EDS reduction signal in the presence of interfering species had an insignificant current drop of only 2.1 % proving the proposed sensor's superior selectivity towards EDS detection.

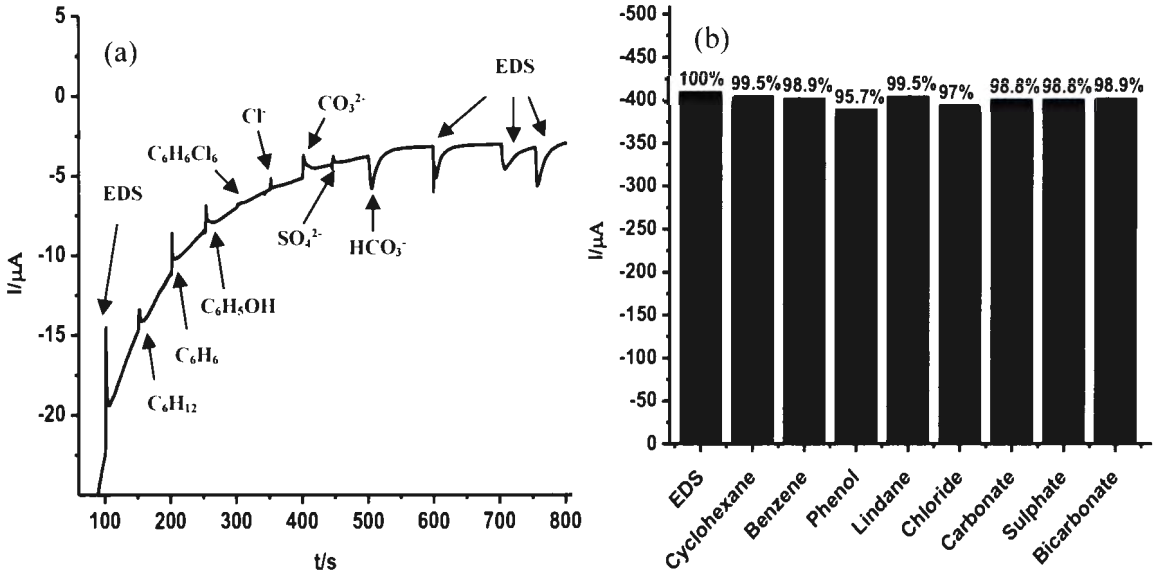

Figure 4.14: (a) Continuous amperometric response at GCE/AONP/PANI/SWCNT modified electrode in the presence of 1 mM interfering species such as cyclohexane, benzene, phenol, lindane, Cl^-, CO_3^{2-}, SO_4^{2-}, and HCO_3^- compared to addition of EDS (b) shows the variation of reduction signal for interfering species with respect to EDS as a percentage by cyclic voltammetry at GCE/AONP/PANI/SWCNT modified electrode in 2:1 water/acetonitrile containing 0.1 M H_2SO_4 at a scan rate of 25 mVs^{-1}.

4.4.5 Endosulfan real sample analysis

Real sample analysis was carried out to establish the practical application of the GCE/AONP/PANI/SWCNT modified electrode towards EDS detection in both river water and tap water samples. The river water samples were collected from upper crocodile sub – catchment of Crocodile River in Rustenburg of the North West province, South Africa at a point with GPS coordinates: S 025° 40' 52.6 E 027° 48' 12.6 and labeled B. The river water was used without further purification. EDS samples with concentrations ranging from 20 μM – 100 μM were prepared in 2:1 tap-water/acetonitrile containing 0.1 M H_2SO_4. SWV experiment were carried out to determine the concentration of EDS in the samples. Results obtained are presented in Table 4.6. The results indicate good recoveries of EDS in the concentration range 20 μM – 100 μM with an average recovery of 99.4 %.

Tap water samples were collected from a residential area Lomanyaneng village, Mahikeng in the North West province of South Africa with GPS coordinates S 25° 54. 251' E 025° 38.412'. The water is supplied by the local municipality and was used without further purification. EDS samples with concentrations ranging from 46 µM – 196 µM were prepared in 2:1 tap-water/acetonitrile containing 0.1 M H_2SO_4. SWV studies were carried out to determine the concentration of EDS in the samples and the results obtained are presented in Table 4.6. The GCE-AONP-PANI-SWCNT modified electrode demonstrated good recoveries (97.5 % average) towards EDS detection in tap water.

Table 4.6: Determination of EDS concentration in river water and tap water samples by SWV.

Sample	Compound	Added (µM)	Found[a] (µM)	Recovery (%)	RSD (%)
River water	EDS	20	19.1	95.5	1.23
		40	40.2	100.5	1.08
		80	83.3	104	2.18
		100	97.5	97.5	1.06
Tap water	EDS	46	42.7	92.9	1.87
		96	96.1	100.1	4.07
		146	145.9	99.9	1.19
		196	190.0	96.9	2.52

[a]Average value of three determination

CHAPTER 5

CONCLUSSIONS AND RECOMENDATIONS

5.1 Conclusions

This work describes the successful fabrication of a sensor for the electrochemical detection of some selected organochlorine pesticides (lindane and endosulfan). The sensor was based on the modification of glassy carbon electrode with various nanomaterials such as AONPs, PANI, fSWCNTs and the nanocomposite AONP-PANI-SWCNT. Characterization of the variously modified electrodes by CV experiments indicated that the GCE-AONP-PANI-SWCNT electrode had better electron transport and catalytic properties in the $[Fe(CN)_6]^{4-}/[Fe(CN)_6]^{3-}$ redox system as compared to the other electrodes investigated. GCE-AONP-PANI-SWCNT electrode had higher electroactive surface area (8.34×10^{-4} cm^2) suggesting ease of electron transport on the electrode. From the voltammetric data obtained GCE-fSWCNTs electrode had lower ΔEp value (70.3 mV) supporting numerous literature reports on the proven enhanced electron transport properties of carbon nanotubes, however GCE-AONP-PANI-SWCNT electrode exhibited higher current response (451 µA). Enhanced electrochemical behaviour of GCE-fSWCNTs electrode due to the fSWCNTs was further depicted by the lower charge transfer resistance (R_{ct}) values (25.01 Ω cm^2) which furthermore proved carbon nanotubes to be a good electrode support material.

Electrocatalytic reduction of 9 µM lindane was carried out using CV technique and the reduction peak at the GCE-AONP-PANI-SWCNT electrode was observed at -0.9 V with a reduction current of 267 µM as compared to that of bare GCE 43.5 µM. Stability study (20 scans) was carried out using GCE-AONP-PANI-SWCNT electrode and virtually no current decrease between the 1^{st} and 20^{th} scan was observed. This suggests that fabricated GCE-AONP-PANI-SWCNT sensor is stable and resistant to electrode fouling effects. The effect of scan rate was investigated using CV experiment and the plot of reduction peak currents versus square root of scan rate yielded a linear relationship where reduction current increased simultaneously with increasing scan rate suggesting diffusion controlled process of lindane reduction. The LoD (2.01 nM), LoQ (6.09 nM) and sensitivity (202.5 µA/µM) of the GCE-AONP-PANI-SWCNT electrode towards lindane were determined from the plot of current versus lindane concentrations.

Electrocatalytic reduction of 86 µM EDS was carried out using CV method and the reduction peak at the GCE-AONP-PANI-SWCNT electrode was observed at -0.13 V with a large reduction current of -510 µM as compared to that of bare GCE -5.52 µM. The sensor proved

outstandingly stable towards electrode fouling as virtually no current drop was observed during stability study in EDS solution. Scan rate study was conducted by CV and the plot of reduction peak currents versus the square root of scan rate yielded a linear graph defined by equation $I_p = -35.38v^{1/2} - 686.56$ with correlation coefficient of $R^2 = 0.9881$. This relationship suggested a diffusion controlled process for EDS reduction on the electrode. The LoD (5.22 µM), LoQ (15.8 µM) and sensitivity (0.2086 µA/µM) of the GCE-AONP-PANI-SWCNT electrode towards EDS were also determined from the plot of current versus EDS concentration.

The proposed sensor further demonstrated good selectivity and anti-interference behavior towards the detection of the selected OCPs in the presence of some interfering species. Real sample analysis to establish the analytical potential of the developed GCE-AONP-PANI-SWCNT sensor was carried out using river and tap water samples. The percentage recoveries obtained for lindane and EDS concentrations at the fabricated sensor indicates its potential for the determination of the analyte in river and tap water samples.

5.2 Recommendations

- It is imperative that regulatory authorities should regulate and monitor the use of OCPs in the environment. This may include updating current legislature to be on par globally. Furthermore scientific research and particularly more innovative and cost effective methods of pesticide monitoring should be explored.

- The proposed sensor should be developed and manufactured for real application in the environment.

- Future studies should focus on the development of simple but economically cheap and available sensors that can readily detect a broader range of OCPs in a variety of matrices such as water, soil and effluents.

References

1. El-Shahawi, M.S.; Hamza, A.; Bashammakh, A.S.; Al-Saggaf, W.T. *Talana* **2010**, 80, 1587.
2. Jones, K.C.; de Voogt, P. *Environ. Pollut.* **1999**, 100, 209.
3. Chrysikou, L.; Gemenetzis, P.; Kouras, A.; Manoli, E.; Terzi, E.; Samara, C. *Environ. Int.* **2008**, 34, 210.
4. Salihovic, S.; Mattioli, L.; Lindstrom, G.; Lind, L.; Lind, P.M.; Van Bavel, B. *Chemosphere*, **2012**, 86, 747.
5. Van Dyk, J.S.; Pletschke, B. *Chemosphere* **2011**, 82, 291.
6. Gill, S.; Bowers, W.J.; Nakai, J.S.; Yagminas, A.; Mueller, R.; Pulido, O. *Toxicol. Pathol.* **2013**, 41, 38.
7. South Africa. Dept. of Agriculture, Forestry and Fisheries. Pesticide management policy. 33899: Government printers, **2010**. Print.
8. Garrido, E.M.; Delerue-Matos, C.; Lima, J.L.F.C.; Brett, A.M.O. *Anal. Lett.* **2004**, 37, 1755.
9. Wilson, C.; Tisdell, C. *Ecol. Econ.* **2001**, 39, 449.
10. Villa, S.; Vighi, M.; Maggi, R.; Finizio, A.; Bolzacchini, E. *J. Atmos. Chem.* **2003**, 46, 295.
11. Delaware department of health and social services, Organochlorine pesticides www.dhss.delaware.gov. n.d. Web. 8 June 2015.
12. Abdollahi, M.; Ranjbar, A.; Shadnia, S.; Nikfar, S.; Rezaie, A. *Med. Sci. Monit.* **2004**, 10(6) RA141

13. Anirudhan, T.S.; Alexander, S. *Biosens. Bioelectron.* **2015**, 64, 586.

14. Turusov, V.; Rakitsky, V.; Tomatis, L. *Environ. Health Perspect.* **2002**, 110, 125.

15. Fatoki, O.S.; Awofolu, O.R. *J Environ. Sci. Health., Part B* **2004**, B39, 101.

16. Prathap, M.U.A.; Srivastava, R. *Electrochim. Acta* **2013**, 108, 145.

17. Pesticide action network, www.panna.org. n.p. n.d. Web.18 June 2015

18. Saiyed, H.; Dewan, A.; Bhatnagar, V.; Shenoy, U.; Shenoy, R.; Rajomohan, K.P.; Kashyap, R.; Kulkarni, P.; Rajan, B.; Lakkad, B. *Environ. Health Perspect.* **2003**, 111, 1958.

19. Sreekumaran N.A.; Renjis, T.T.; Pradeep, T. *J. Environ. Monit.* **2003**, 5, 363.

20. United States. Dept. of health and human services. Agency for toxic substances and disease registry. Public health service. Draft toxicological profile for endosufan. 3033, Atlanta Georgia, **2013**. Print.

21. Schmidt, W.F.; Hapeman, C.J.; Fettinger, J.C.; Rice, C.P.; Bilboulian, S. *J. Agr. Food Chem.* **1997**, 45, 1023.

22. Mathava, K.; Ligy, P. *J Environ. Sci. Health., Part B* **2006**, 41, 81.

23. Mathava, K.; Ligy, P. *Bioremediat. J.* **2006**, 10(4), 179.

24. Balzani, V. *Small*, **2005**, 3, 278.

25. Mohanraj, V.J.; Chen, Y. *Trop. J Pharm. Res.* **2006**, 5(1), 561.

26. Silwana, B.; Van der Horst, C.; Iwuoha, E.; Somerset, V. *Thin Solid Films*, **2015**, 592, 124.

27. Zhang, L.; Fang, M. *Nanotoday*, **2010**, 5, 128.

28. Salimi, A.; Mamkhezri, H.; Hallaj, R.; Soltanian, S. *Sensor. Actuat. B Chem.* **2008**, 129, 246.

29. Grosan, C.B.; Varodi, C.; Vulcu, A.; Olenic, L.; Pruneanu, S.; Almasan, V. *Electrochim. Acta* **2012**, 63, 146.

30. Mailu, S.N.; Waryo, T.T.; Ndangili, P.M.; Ngece, F.R.; Baleg, A.A.; Baker, P.G.; Iwuoha, E.I. *Sensors*, **2010**, 10, 9449.

31. Chen, H.; Zhang, Z.; Cai, R.; Rao, W.; Long, F. *Electrochim. Acta* **2014**, 117, 385.

32. Fayemi, O.E.; Adekunle, A.S.; Ebenso, E.E. *J. Biosens. Bioelectron.* **2015**, 6, 4.

33. Habibi, B.; Jahanbakshi, M. *Electrochim. Acta* **2014**, 118, 10.

34. Baciu, A.; Pop, A.; Manea, F.; Schoonman, J. *Environ. Eng. Manag. J.* **2014**, 13, 2317.

35. Wang, P.; Mai, Z.; Dai, Z.; Li, Y.; Zou, X. *Biosens. Bioelectron.* **2009**, 24, 3242.

36. Huang, X.; Li, Y.; Chen, Y.; Wang, L. *Sensor. Actuat. B. Chem.* **2008**, 134,780.

37. Xu, X.; Duan, G.; Li, Y.; Liu, G.; Wang, J.; Zhang, H.; Dai, Z.; Cai, W. *Appl. Mater. Interfaces* **2014**, 6, 65.

38. Prathap, A.M.U.; Sun, S.; Xu, Z.J.; *RCS adv.* **2016**, 6, 22973.

39. Fayemi, O.E.; Adekunle, A.S.; Ebenso, E.E.; *J. Nanomater.* **2016**, 2016, 78

40. Cesarino, I.; Cesarino, V.; Marcos, R.V.L. *Sensor. Actuat. B. Chem.* **2013,** 188, 1293.

41. Moraes, F.C.; Cesarino, I.; Cesarino, V.; Mascaro, H.L.; Machado, S.A.S. *Electrochim. Acta* **2012**, 85, 560.

42. Chin, H.S.; Cheong, K.Y.; Razak, K.A. *J. Mater. Sci.* **2010**, 45, 5993.

43. Zhang, Z.; Guo, L.; Wang, W. *J. Mater. Res.* **2001**, 16(3), 803.

44. Zeng, D.W.; Xie, C.S.; Zhu, B.L.; Song, W.L. *Mater. Lett.* **2004**, 58, 312.

45. Jha, A.K.; Prasad, K.; Prasad, K. *Biochem. Eng. J.* **2009**, 43, 303.

46. Kroto, H.W.; Heath, J.R; O'Brien, S.C.; Curl, R.F.; Smalley, R.E. *Nature* **1985**, 318, 162.

47. Eatemadi, A.; Daraee, H.; Karimkhanloo, H.; Kouhi, M.; Zarghami, N.; Akbarzadeh, A.; Abasi, M.; Hanifehpour, Y.; Joo, S.W. *Nanoscale Res. Lett.* **2014**, 9, 393.

48. Thostenson, E.T.; Ren, Z.; Chou, T. *Compos. Sci. Technol.* **2001**, 61, 1899.

49. Bonalume, B.C.F.; Lebrao, G.W.; Rossi, J.L. 16th international conference on composite structures **2011**.

50. Joseph, Wang. *Electrochemical sensors for environmental monitoring*. New Mexico state university. Las Cruses. **2004**. Print.

51. Notarianni, M.; Liu, J.; Vernom, K.; Motta, N. *Beilstein J. Nanotechnol.* **2016**, 7,

52. Vairavapandian, D.; Vichulada, P.; Lay, M.D. *Anal. Chimi. Acta* **2008**, 626, 119.

53. Adekunle, A.S.; Mamba, B.B.; Agboola, B.O.; Ozoemena, K.I. *Int. J. Electrochem. Sci.* **2011**, 6, 4388.

54. Adekunle, A.S.; Agboola, B.O.; Pillay, J.; Ozoemena, K.I. *Sensor. Actuat. B-Chem.* **2010**, 148, 93.

55. Adekunle, A.S.; Pillay, J.; Ozoemena, K.I. *Electrochim. Acta*,**2010**, 55, 4319.

56. Gerard, M.; Chaubey, A.; Malhotra, B.D. *Biosens. Bioelectron.* **2002**, 17, 345.

57. Tovide, O.; Jaheed, N.; Mohamed, N.; Nxusani, E.; Sunday, E.C.; Tsegaye, A.; Ajayi, F.R.; Njomo, N.; Makelane, H.; Bilibana, M.; Baker, P.G.; Williams, A.; Vilakazi, S.; Tshikhudu, R.; Iwuoha, E.I. *Electrochim. Acta* **2014**, 128, 138.

58. Trchová, M.; Stejskal, J. *Pure Appl. Chem.* **2011**, 83(10), 1803.

59. Yu, Q.-Z.; Shi, M.-M.; Deng, M.; Wang, M.; Chen, H.-Z. *Mat. Sci. Eng. B-Solid*, **2008**, 150, 70.

60. Dalui, B.C.; Basumallick, I.N.; Ghosh, S. *Indian J. Chem. Technol.* **2008**, 15, 576.

61. Sairam, M.; Nataraj, S.K.; Aminabhavi, T.M.; Roy, S.; Madhusoodana, C.D. *Sep. Purif. Rev.* **2006**, 35, 249.

62. Prathap, M.U.A.; Srivasta, R. *J. Polym. Res.* **2011**, 18, 2455.

63. Zhang, L.; Su, K.; Li, X. *J. Appl. Polym. Sci.* **2002**, 87(5), 733.

64. Rahman, M.A.; Kumar, P.; Park, D.-S.; Shim, Y.-B. *Sensors*, **2008**, 8, 118.

65. Stradiotto, N.R.; Yamanaka, H.; Zanoni, M.V.B. *J. Braz. Chem. Soc.* **2003**, 14(2), 159.

66. Rahman, M.A.; Kumar, P.; Park, D.S.; Shim, Y.B. *Sensors*, **2008**, 8, 118.

67. Prathap, A,M.U.; Sun, S.; Wei, C.; Xu, Z.J. *Chem. Commun.* **2015**, 51, 4379.

68. Otles, S. *Handbook of food analysis instruments*; CRC Press, 2016; Chapter 17.

69. Skoog, D.A.; Holler, J.; Crouch, S.R. *Principles of instrumental analysis*; Cengage learning, 2017; Chapter 25.

70. Settle, F.A. *Handbook of instrumental techniques for analytical chemistry*; Prentice Hall PTR, 1997; Chapter 37.

71. Culebras, M.; Gómez, C.M.; Cantarero, A. *Materials*, **2014**, 7, 679.

72. Compton, R.G.; Laborda, E.; Ward, K.R. *Understanding voltammetry: Simulation of electrode processes*, Imperial college press, 2014; Chapter 2.

73. Lehmann, K.; Yurchenko, O.; Urban, G.A. *J. Phys. Conf. Ser.* **2014**, 557, 012008.

74. Mirceski, V.; Gulaboski, R.; Lovric, M.; Bogeski, I.; Kappl, R.; Hoth, M. *Electroanalysis*, **2013**, 25(11), 2411.

75. Mirceski, V.; Gulaboski, R. *Maced. J. Chem. Eng.* **2014**, 33(1), 1.

76. Lasia, A. *Electrochemical impedance spectroscopy and its applications*, Kluwer academic/Plenum publishers, 1999, 143.

77. Lisdat, F.; Shäfer, D. *Anal. Bioanal. Chem.* **2008**, 391, 1555.

78. Randviir, E.P.; Banks, C.E. *Anal. Methods*, **2013**, 5, 1098.

79. Kavitha, B.; Kurma, K.S.; Narsimlu, N. *Indian J Pure & Appl. Phys.* **2013**, 51, 207.

80. Tchoul, M.N.; Ford, W.T; Lollo, G.; Resasco, D.E.; Arepalli, S.; *Chem. Mater.* **2007**, 19(23), 5765.

81. Adekunle, A.S.; Mamba, B.B.; Agboola, B.O.; Ozoemena, K.I. *Int. J. Electrochem. Sci.* **2011**, 6, 4388.

82. Kaviyarasu, K.; Sajan, D.; Devarajan, P.A. *Appl. Nanosci.* **2013**, 3, 529.

83. Abdolahi, A.; Hamzah, E.; Ibrahim, Z.; Hashim, S. *Materials*, **2012**, 5, 1487.

84. Prathap, M.U.A.; Srivastava, R.; Satpati, B. *Electrochim. Acta*, **2013**, 114, 285.

85. Olad, A.; Ilghami, F.; Nosrati, R. *Chemical papers*, **2012,** 66(8), 757.

86. Cesarino, I.; Moraes, F.C.; Machado, S.A.S. *Electroanalysis*, **2011**, 23(11), 2586.

87. Helali, S.; Bohli, N.; Mostafa, H.M.A.; Zina, H.B.; Al-Hartomy, O.A.; Abdelghani, A.; *J. Nanomed. Nanotechnol.* **2016**, 7(4), 100396.

88. Xu, K.; Lin, W.; Wu, J.; Peng, J.; Xing, Y.; Gao, S.; Ren, Y.; Chen, M. *New J. Chem.* **2015**, 39, 8405.

89. Khalef, W.K. *Iraqi journal of applied physics*, **2013**, 9(3), 13.

90. Konyushenko, E.N.; Reynard, S.; Pellerin, V.; Trchová, M.; Stejskal, J.; Supurina, I.; *Polymer*, **2011**, 52, 1900.

91 Chiang, I.W.; Brinson, B.E.; Smalley, R.E.; Margrave, J.L.; Hauge, R.H. *J. Phys. Chem. B*, **2001**, 105, 1157.

92. Peng, H.; Alemang, L.B.; Margrave, J.L.; Khabasheski, V.N. *J. AM. Chem. Soc.* **2003**, 125(49), 15177.

93. Price, B.K.; Tour, J.M. *J. AM. Chem. Soc.* **2006**, 128, 12899.

94. Ng, S.H.; Wang, J.; Guo, Z.P.; Chen, J.; Wang, G.X.; Liu, H.K. *Electrochim. Acta,* 2005, 51, 23.

95. Liu, G.; Wang, S.; Liu, J.; Song, D. *Anal. Chem.* **2012**, 84, 3921.

96. Adekunle, A.S.; Lebogang, S.; Gwala, L.P.; Tsele, T.P.; Olasunkanmi, L.O.; Fayemi, O.E.; Boikanyo, D.; Mphuthi, N.; Oyekunle, J.A.O.; Ogunfowokan, A.O.; Ebenso, E.E. *RSC. Adv.* **2015**, 5, 27759.

97. Grewal, Y.S.; Shiddiky M.J.A.; Gray, S.A.; Weigel, K.M.; Cangelosi, G.A.; Trau, M. *Chem. Commun.* **2013**, 49, 1551.

98. Bard, A.J.; Faulkner, L.R. *Electrochemical methods: Fundamentals and applications*, John Wiley and Sons, 2001, Chapter 10.

99. Kaur, B.; Srivastara, R.; Satpati, B. *RSC Adv.* **2015**, 5, 57657.

100. Kumaravel, A.; Vincent, S.; Chandrasekaran, M. *Anal. Methods*, **2013**, 5, 931.

101. Hegde, R.N.; Swamy, B.E.K.; Sherigara, B.S.; Nandibewoor, S.T. *Int. J. Electrochem. Sci.* **2008**, 3, 302.

102. Siswana, M.; Ozoemena, K.I.; Nyokong, T. *Talanta*, **2006**, 69, 1136.

103. Isse, A.A.; Gottardelo, S.; Durante, C.; Gennaro, A. *Phys. Chem. Chem. Phys.* **2008**, 10, 2409.

104. Adekunle, A.S.; Ozoemena, K.I. *Electroanalysis*, **2010**, 22(21), 2519.

105. Singh, S.N. *Microbe-induced degradation of pesticides*, Springer International Publishing, 2016.

106. Priyantha, N.; Thirana, S.M. *Ceylon J. Sci. Phys. Sci*, **1999**, 6(1), 38.

107. Ribeiro, F.W.P.; Oliveira, T.M.B.F.; da Silva, F.L.F.; Mendonça, G.L.F.; Homem-de-Mello, P.; Becker, H.; de Lima-Neto, P.; Correia, A.N.; Freire, V.N. *Microchem. J.* **2013**, 110, 40.

108. Bow, Y.; Sutriyono, E.; Nasir, S.; Iskandar, I. *Int. J. Sci. Engg. Tech.* **2017**, 7(2), 662.

APPENDICES

Formulae used:

Δ Ep : $\Delta Ep = Epc - Epa$

$E_{1/2} = \frac{E\,pc + E\,pa}{2}$

$I_p = 2.69 \times 10^5 n^{3/2} AC\sqrt{Dv}$

$LoD = 3.3\,{}^{\delta}/_{m}$